



Artificial Recharge of an Unconfined Aquifer Using Treated Wastewater as a Climate Change Mitigation Strategy

Rana A. H. Mukheef^{1,2}, Waqed H. Hassan^{3,4*} , S. Alquzweeni² 

¹ Civil Engineering Department, College of Engineering, Al-Qasim Green University, Babylon, 51013, Iraq.

² Civil Engineering Department, College of Engineering, University of Babylon, Babylon, Iraq.

³ College of Engineering, University of Warith Al-Anbiyaa, Kerbala 56001, Iraq.

⁴ Department of Civil Engineering, College of Engineering, University of Kerbala, Kerbala 56001, Iraq.

Received 12 October 2024; Revised 11 December 2024; Accepted 21 December 2024; Published 6 January 2025

Abstract

Worldwide groundwater extraction has increased dramatically during the past six decades. Water scarcity will affect 1.4 billion people in around 48 nations by 2025. Iraq is experiencing an unparalleled and severe water crisis due to various factors, including climate changes, insufficient rainfall, the policies of neighboring nations, and the increased demand resulting from population expansion. The research area (Dibdiba aquifer) is in Iraq, in the middle between Najaf and Karbala. It was observed that farmers had abandoned numerous wells as a result of the decline in their water levels. Groundwater is the water resource for the region, and due to high agricultural and industrial demand, the Dibdiba aquifer is facing groundwater depletion. This study utilized climatic datasets projected under two scenarios obtained from CMIP6 and the Groundwater Modeling System (GMS). The objective was to evaluate the effect of projected climate change on the quantity of groundwater. Artificial recharge of treated wastewater from the wastewater treatment plant (WWTP) in Kerbala into groundwater aquifers has proven to be an effective method of mitigating groundwater depletion while providing a sustainable water supply. Eleven wells are distributed randomly within the research area; each of them is located within the unconfined aquifer. The groundwater levels in these wells were measured in situ from July 2023 to April 2024. The model was run for steady and unsteady flow conditions, and calibration at steady state was carried out using the groundwater head data for (7) wells. These seven wells were selected to represent the whole research region as well as shorten the simulation run duration in the calibration process. On the other hand, the transient calibration was performed employing measurements of groundwater heads for four wells. Calibration and validation results indicated convergence between the observed and simulated heads. The modeling findings showed that the increment in groundwater level is about 1.0, 1.85, and 2.25 m with artificial recharge of about 6000 m³/day, 9000 m³/day, and 12000 m³/day, respectively. The above findings illustrate the ability of artificial recharge as a highly promising strategy for addressing the water depletion and environmental issues in the Dibdiba aquifer.

Keywords: Climate Change; Artificial Recharge; GMS Software; Dibdiba Aquifer.

1. Introduction

Groundwater, for many aquifers of the world, is considered a reliable resource for human requirements if it is protected from contamination [1]. It is an optimal water source due to its stability over prolonged durations and extensive areas and is not as susceptible to long-term and seasonal fluctuations. In the lack of alternative water sources, like lakes

* Corresponding author: waqed.hammed@uowa.edu.iq; waqed2005@yahoo.com

 <http://dx.doi.org/10.28991/CEJ-SP2024-010-016>



© 2024 by the authors. Licensee C.E.J, Tehran, Iran. This article is an open access article distributed under the terms and conditions of the Creative Commons Attribution (CC-BY) license (<http://creativecommons.org/licenses/by/4.0/>).

or rivers, groundwater often serves as a viable choice [2, 3]. It is important for many purposes, involving drinking, farming, industry, ecosystems, and the environment [4-7]; it helps to address the water supply shortage caused by malfunctioning infrastructure. The water supply must meet particular quality standards to guarantee safe consumption, determined by the physical-chemical composition of groundwater, which is regulated by several hydrochemical processes, including dissolution, evaporation, precipitation, and oxidation-reduction [8]. The growing utilization of groundwater for irrigation and human use resulted in a decrease in underground water levels in many regions worldwide. Groundwater demand is rising quickly due to an increase in human activities. Anthropogenic stress on water supplies has increased due to rapid population expansion worldwide and rising global water demand [9-11].

Groundwater plays a crucial role in the climatic system, as emphasized by Asadi et al. [5]. The myriad potential impacts of climate change on groundwater remain unclear due to the detailed architecture of the climatic system, characterized by feedback mechanisms and intricate interconnections [12]. Climate change has created issues and crises in every part of the world in recent years. A global concentration of greenhouse gases, involving nitrous oxide, methane, and CO₂, has significantly grown due to economic growth and population development. According to projections, the temperature is anticipated to increase by 3.30 to 5.70 °C in the (2081-2100) and by 1.5 °C shortly 2021-2040 under the most severe emission scenario, according to the IPCC's Sixth Assessment Report [13]. Temperature increases can markedly affect hydrological processes by increasing the transpiration of plants and the evaporation of surface water. These alterations are anticipated to affect rainfall patterns, intensity, and timing, indirectly affecting the distribution and water storage in surface and groundwater reservoirs, including lakes, groundwater, and soil moisture (IPCC, 6th Assessment Report). As opposed to surface water resources, groundwater resources are more slowly and indirectly influenced by climate change; it is necessary to monitor the condition of these sources and ensure their sustainability in the face of these changes [14].

The correlation between groundwater resources and climate change needs to be better understood. The water balance method is widely employed for determining groundwater recharge; however, numerous studies have utilized the empirical rainfall-runoff method to investigate the impacts of climate change on GW. Utilizing climate change-derived inputs to simulate the groundwater system is an effective approach for comprehending the influence of anticipated climate change on GW sources [15].

Iraq is regarded as one of the Middle Eastern countries most vulnerable to the impacts of climate change. Global warming and climate change might directly or indirectly affect groundwater resources. Groundwater water levels, discharge, recharge, and annual storage will all be directly impacted by rising temperatures and shifting precipitation patterns. Furthermore, the quality of groundwater sources may be indirectly affected by increased need for irrigation water, rising sea levels, and changes in vegetation cover. Diurnal variations in evaporation rates and plant transpiration, which indicate soil dryness, will result from global warming, increasing soil moisture losses and decreasing naturally occurring groundwater recharge. Variations in precipitation timing at different time scales can impact groundwater replenishment. Recharge requires sufficient water to penetrate the unsaturated zone to tensile demands and surpass evapotranspiration between the land surface and the water table [16]. Climate change on earth could affect groundwater quality and quantity. According to scientific consensus, the earth's climate has undergone alterations and will keep on changing because greenhouse gas quantities in the atmosphere are rising [16]. Climate change's effect on GW is significant in semiarid and arid regions, as GW typically serves as the primary freshwater resource.

Even at the local level, assessing how groundwater recharge responds to climate change is challenging; one explanation is that groundwater recharge is infrequently studied, unlike stream flow, and extensive time series of groundwater recharge data are lacking. In local groundwater simulation, groundwater recharge is often calibrated employing hydraulic head observations. Integrated simulating depends on the division of rainfall into evapotranspiration, changes in runoff (including surface and subsurface runoff and groundwater recharge), and storage. Furthermore, forecasts of groundwater recharge often ignore the effect of climate change and higher concentrations of CO₂ on vegetation and, thus, on evapotranspiration and groundwater recharge [17].

Artificial recharge technology can increase groundwater supplies, which includes applying water from the surface to the ground or injecting water underground. It is a human-made process that enables surface water infiltration into aquifers. Several methods facilitate the transfer of surface water to subsurface formations. The objectives of artificial recharge involve groundwater management, land subsidence prevention, wastewater reclamation, and improvement of groundwater quality during sharp reductions in surface water flow and flooding events. Artificial recharge projects also contribute to water conservation. A practical artificial recharge project includes two essential components: a dependable source of high-quality water and a comprehensive understanding of the subsurface geological and hydrological conditions [18]. It can be done even when freshwater resources from traditional sources are limited. Treated wastewater can serve as an alternative resource for irrigation to fulfill agricultural water requirements and for the artificial recharge

to mitigate groundwater depletion. Many countries, including France, Saudi Arabia, the United States of America, Cyprus, the Netherlands, Qatar, Canada, Brazil, Mexico, China, India, and Egypt, employ such approaches. Artificial recharge is a method for sustainably managing the depletion of groundwater levels in countries such as Iraq, which are situated in arid areas. The two most popular techniques for artificial recharge are pond water filtration and well pumping. Wells were used in this study to replenish the aquifer because of the significant amounts of raw water lost and the increased evaporation rate in these surface water ponds compared to wells [10].

Several investigations have been done on the effect of climate change and variation in levels of groundwater in the Dibdiba aquifer. Hassan & Hashim [19] examine climate change's impact on groundwater recharging in aquifers in the Karbala–Najaf region. The outcomes of this research indicated that groundwater recharge decreased by 6.4%, 10%, and 27.6% for the near future and by 13.6%, 17.6%, and 25.3% for the far future, compared to the year 2018 under RCP scenarios of 2.6, 4.5, and 8.5, respectively. Hussain et al. [20] used the groundwater modeling system (GMS) to simulate groundwater in the Karbala Governorate. The research region was about 2400 km², which contains about 22 wells dispersed across the research region, and whose discharge varies from 7 to 100 l/s and up to 36 l/s. They found that for three years, the model was developed in the sight of the above wells, and the findings showed a uniform decrease in groundwater levels of between 2 and 21 meters across the study area. Khalaf et al. [21] employed GMS to assess the influence of artificial recharge on aquifer groundwater levels. The effluent from Kerbala's principal wastewater treatment facility, equipped with 20 injection wells, became the primary raw water source for the artificial recharge process. The statistics demonstrate that water treated via injection through twenty wells raised the water level in regions above 91 km² and 136 km² for pumping rates of 5000 m³/day and 10,000 m³/day, respectively. Furthermore, enhancing the aquifer's water supply might create a new agricultural zone beyond 62 km², stretching around twenty km along the river.

Although there has been a rise in studies regarding the effects of global warming on groundwater in recent years, additional study is essential to mitigate the impact of climate change on groundwater in Iraq. This study aims to fill the research vacuum by examining the effects of climate change on groundwater and alleviating these effects through artificial recharge techniques. Overall, this comprehensive review has illuminated the far-reaching consequences of climate change on the vulnerability and sustainability of groundwater and global warming mitigation methods. It is necessary that researchers recognize the indispensable role of groundwater in sustaining ecosystems, agriculture, and populations. This review not only serves as a call to action but also as a guide for informed decision-making to secure a more resilient future for groundwater resources.

This research evaluates the effects of global warming on GWR utilizing the bias-adjusted results from three GCMs over two distinct Shared Socioeconomic Pathways (SSPs) in the aquifer located in the Karbala Governance in central Iraq during the next few decades. It assesses the influence of artificial recharging groundwater levels.

2. Research area

2.1. Overview of Study Area

The research region, the Dibdiba aquifer, is located between Najaf and Karbala in central Iraq. It is situated within the latitudes 31° 55'N to 32° 45'N and longitudes 43° 50'E to 44° 30'E, as illustrated in Figure 1. The Dibdiba is an unconfined aquifer, meaning any confining layers do not restrict it. This renders it more susceptible to climate change effects, as the Dibdiba aquifer is located close to the surface and covers an area of 1100 km² [22]. The formation is revealed on the Tar Al-Sayid and Tar Al-Najaf ridges. The bedrock of the desert plain between Najaf and Karbala constitutes the region's principal part of the exposed sequence [23]. Razzaza Lake, a surface reservoir, is situated in the northern area of the subsurface water reservoir. To the east, the aquifer is defined by quaternary strata. The aquifer is regarded as one of the most significant in Iraq. Extends from the central region to the southernmost part of the country. Recharge of Al Dibdiba relies on precipitation, which is influenced by variations in temperature [22].

In the Mesopotamian Basin, the seasonal flow of streams was directed at 40°N. The early Miocene creation of the Dibdiba alluvial fan delta is ascribed to the drainage system evident upstream on the carbonate platform of the Western Desert [24]. The Dibdiba formation comprises sandstone, pebbly sandstone, siltstone, claystone, and marl associated with secondary gypsum. The formation has a thickness of 45–60 meters. The area under study is characterized by sandy soil, which increases percolation and infiltration rates for irrigation. The groundwater in the area is stored within the Dibdiba Formation, which is of the Pliocene era. Approximately 84% of the groundwater used for irrigation would quickly return to the unconfined aquifer, and each year about 25 mm of precipitation would recharge the groundwater (with a minimal amount of 15% being recharged to the groundwater) [25]. Table 1 reports the longitudes and latitudes of selected wells in the research region.

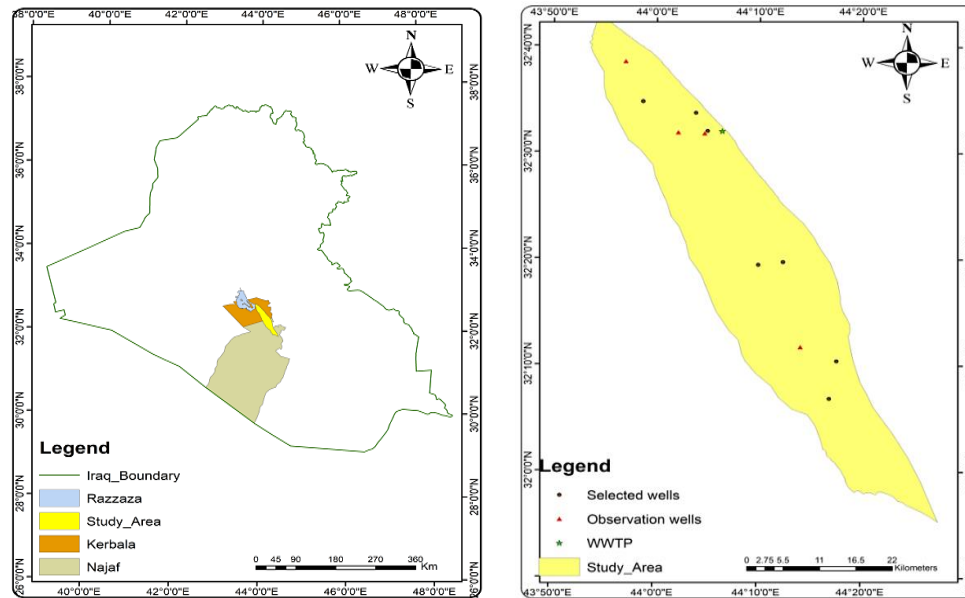


Figure 1. Research area location

Table 1. Mean monthly precipitation and temperatures at the Karbala and Najaf meteorological stations

Months	Temperature (⁰ C)		Precipitation (mm)	
	Karbala	Najaf	Karbala	Najaf
Jan.	10.40	10.52	13.66	19.27
Feb.	12.82	13.01	12.38	10.51
Mar.	17.44	17.78	11.06	12.24
Apr.	23.95	24.33	8.09	9.69
May	30.39	30.67	6.29	3.18
Jun.	35.02	35.11	0.04	0.02
Jul.	37.45	37.45	0	0
Aug.	37.26	37.28	0	0
Sep.	33.47	33.56	0.01	0.01
Oct.	27.49	27.62	1.81	3.14
Nov.	15.901	16.05	6.70	12.46
Dec.	12.37	12.47	17.14	10.16
Average	24.50	24.66		
Total			77.16	80.67

2.2. Hydrogeological Description

Understanding the significance of the relevant flow operations requires an accurate hydrogeological description in the aquifer under investigation. An accurate depiction of the region makes it possible to select a proper model or establish a reliable, calibrated one. The hydrogeological properties of the modeled region, including the aquifer parameters, are only known for a limited number of situations within the research area. Figure 1 displays the positions of the chosen production wells for forecasting the research region's aquifer properties. The precision of aquifer recharge estimation is considerably affected by these characteristics. The most significant characteristics of the soil are the major factors controlling the infiltration flow rate and downward percolation, particularly with this kind of method. Figure 2 illustrates the lithological formation determined using data from deep well logs and infiltration tests. The stratigraphic column in the research region comprises several layers arranged in chronological order from oldest to youngest. These formations include the middle-late Eocene formation known as Al-Dammam, the late lower Miocene formation called Euphrates, the middle Miocene formations known as Nfayil and Fatha, the upper Miocene formation called Injana, and finally the upper Miocene-Pliocene formation known as Dibdiba. The last formation is known as Al-Dibdiba. The seasonal stormwater that falls on the plateau and recharges the aquifer comes from rainfall directly in the eastern and northeastern regions [26].

Era	Period	Epoch	Age	Formation	Lithology	
CENOZOIC	Quaternary	Holocene		Aeolian deposits	[Pattern]	
				Valley fill deposits	[Pattern]	
				Depression deposits	[Pattern]	
			Pleistocene		Gycrete deposits	[Pattern]
	Tertiary	Pliocene		Dibdibba	[Pattern]	
				Injana	[Pattern]	
		Miocene	Upper		Fatha	[Pattern]
			Middle		Euphrates	[Pattern]
						[Pattern]
			Lower			[Pattern]

Figure 2. Lithology and stratigraphy of the formations in the research region

2.3. Climate

Iraq possesses an arid, warm climate characterized by prolonged, sweltering summers and brief, frigid winters. The geographical location between the humid subtropical climate of the Arabian Gulf and the arid subtropical climate of the Arabian Desert significantly influences Iraq's climate. In the majority of regions, summers are hot and mostly sunny. During the summer, air temperatures can be sweltering and accompanied by low humidity. Hot desert winds can be powerful, sometimes having the potential to generate intense sandstorms [26]. The monthly averages of climatic parameters at two meteorological stations in the research region (Karbala and Najaf) stations from 1983 to 2022 are illustrated in Table 1.

Temperature is the primary variable affecting the climate. Latitude, surface characteristics, and prevailing winds influence it. Several factors, including industrial expansion, population expansion and greenhouse gas emissions, have increased temperatures [26]. From 1983 to 2022, the Karbala station exhibited elevated average temperatures in the warmer months of June, July, and August, with July recording the peak average monthly temperature of 37.45⁰ C at both the Najaf and Karbala stations. The average monthly temperature decreases in the cold months of December, January, and February. The average monthly minimum temperatures for January were 10.40⁰ C and 10.52⁰ C for Karbala and Najaf stations, respectively, as shown in Figure 3.

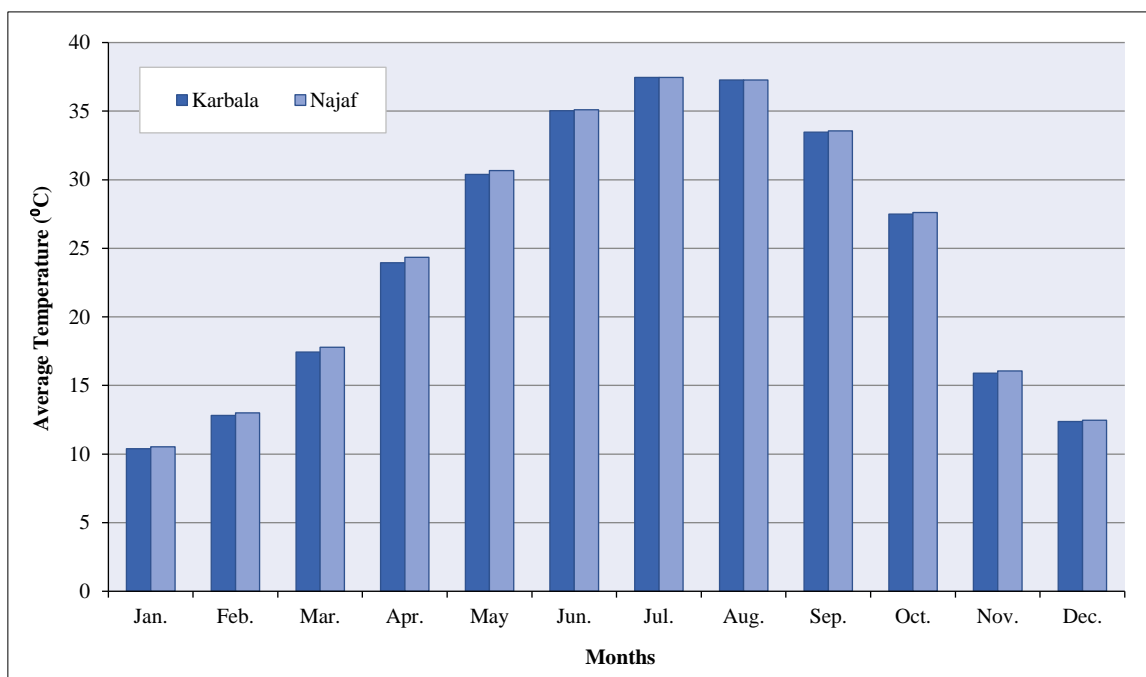


Figure 3. Average monthly temperature for the baseline period (1983-2022) at Karbala and Najaf stations

Precipitation is significant in recharging groundwater aquifers, exceptionally shallow ones. Precipitation is vital to assessing surface and subsurface water resources in the given area. Unlike other climatic parameters, Precipitation is a non-continuous function with random occurrences [27]. Monthly and annual variations are apparent in precipitation,

with the wet season beginning in December (at 17.14 and 10.16 mm) and continuing through to March (at 11.06 and 12.24 mm), with the maximum precipitation recorded in December (17.14 mm) for Karbala station, and in January (19.27 mm) for Najaf station. The period of drought from July (0) mm to August (0) mm for both the Najaf and Karbala stations, as shown in Figure 4.

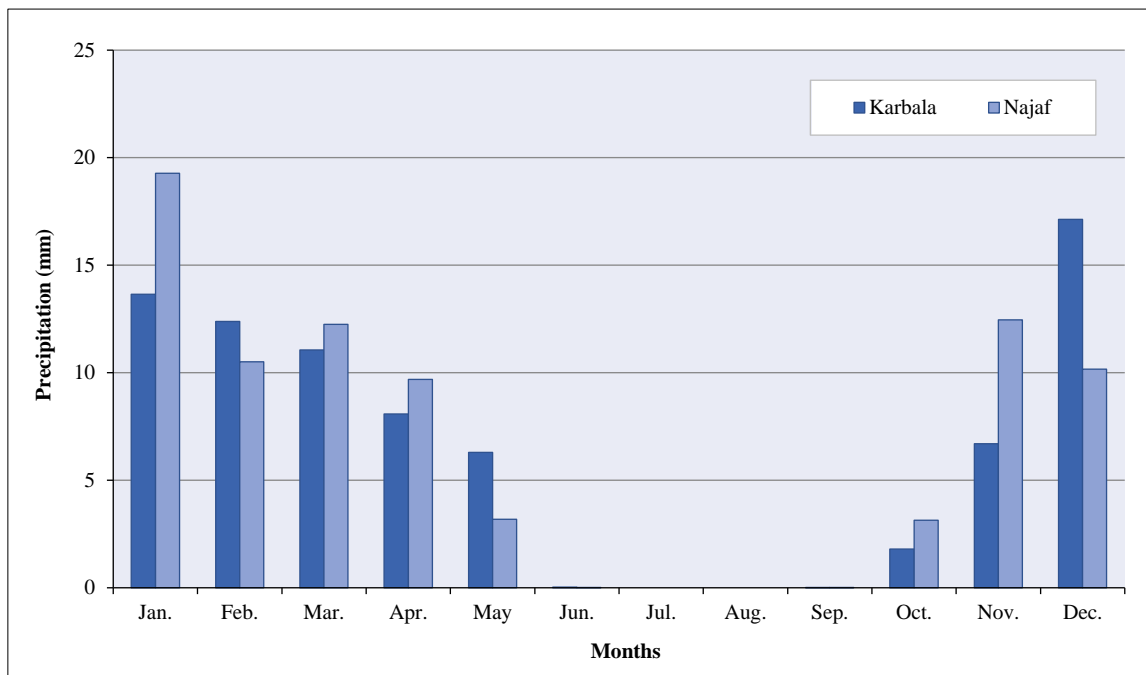


Figure 4. Average monthly precipitation for the baseline period (1983-2022) at Karbala and Najaf stations

2.4. Climate Classification

Various techniques can be used to identify the prevalent climatic type by analyzing different specific coefficients, such as those associated with the variables of aridity and humidity [28]. The climatic classification proposed by Al-Kubaisi [28] can be used to determine the climatic classification by calculating the yearly dryness based on the combination of Precipitation and temperature, as described by the following Equations:

$$AI - 1 = 1 \times \frac{P}{(11.53 * T)} \tag{1}$$

$$AI - 2 = \sqrt{\frac{P}{T}} \tag{2}$$

AI - 1 is Aridity Index, P is Annual precipitation (mm), T is Temperature (°C) and $t \neq 0$.

The value of AI - 1 facilitates the categorization of the existing climate, whereas AI - 2 signifies an alteration of that classification. Utilizing Equations 1 and 2 to ascertain the dominant climatic type in the studied area, AI - 1 and AI - 2 can be determined as follows:

$$AI - 1 = 0.28$$

Comparing this result with the climatic categorization in Table 2, the region's climate is categorized as sub-arid to arid.

Table 2. PE_c for temperature ≥ 26.5 °C [23]

T (°C)	26.5	27	27.5	28	28.5	29	29.5	30	30.5	31	31.5	32
PE (mm)	135	139.5	143.7	147.8	151.7	155.4	158.9	162.1	165.2	168	170.7	173.1
T (°C)	32.5	33	33.5	34	34.5	35	35.5	36	36.5	37	37.5	38
PE (mm)	175.3	177.2	179	180.5	181.8	182.9	183.7	184.3	184.7	184.9	185	185

$$AI - 2 = 1.79$$

Additionally, the area under this classification has a dominant sub-arid climate type when comparing this value with those in Table 3.

Table 3. The climate classification

Type1	Assessment	Type 2	Assessment
AI-1 > 1.0	Humid to moist	AI-2 > 4.5	Humid
		2.5 < AI-2 < 4.0	Humid to moist
		1.85 < AI-2 < 2.5	Moist
		1.5 < AI-2 < 1.85	Moist to sub-arid
AI-1 < 1.0	Sub-arid to arid	1.0 < AI-2 < 1.5	Sub-arid
		AI-2 < 1.0	Arid

3. Research Methodology

3.1. Data Collection

Data were gathered from two precipitation measurement sites in the study area: Karbala and Najaf. The existing rainfall gauges must deliver thorough daily data and frequently exhibit information shortcomings. Consequently, researchers often utilize an alternative source of precipitation data. A CHIRP supplies daily precipitation data for all four research stations employed in this investigation. NASA Power supplies the daily, fluctuating maximum and lowest temperatures for global energy resources (<https://power.larc.nasa.gov/data-accessviewer>) utilized in this study. This research utilized three CMIP6 General Circulation Models for the baseline period from 1983 to 2022. The CMIP6 climate model ensemble was utilized to analyze fluctuations in temperature and precipitation for both the present and future under (SSP2 -4.5) and (SSP5 -8.5) scenarios. The datasets were obtained from the CMIP6 database, which is available online (<https://esgfnode.llnl.gov/search/cmip6>). In investigating the variation in groundwater levels, eleven wells distributed over the aquifer in the research region, from 2023 through 2024 were used. The groundwater level in these wells was measured with a depth-measuring instrument (water sounder). The research region's elevation data was obtained using the Digital Elevation Model (DEM) and processed employing GIS software. The study by Al-Ghanimy [24] served as the basis for the initial specific yield and hydraulic conductivity values.

3.2. Climate Change

This research investigates future climate change in the aquifer employing three General Circulation Models (GCM) and two scenarios: SSP2-4.5 and SSP5-8.5 from the IPCC. The historical data were employed from 1983 to 2022 from two meteorological stations, Karbala and Najaf. The output of GCMs was biased and corrected employing the Climate Model Data for Hydrologic Modelling (CMhyd) program. CMhyd was established to provide bias correction for simulated climate data produced by RCMs and GCMs. The tool has been utilized for bias correction of rainfall and temperature in many applications [29]. CMhyd created simulated climatic data representing the gauge locations employed in a watershed model setup. Therefore, for each gauge location, the climate model data must be extracted and applied to bias correction.

The fundamental concept entails identifying differences between observed and simulated climate variables to parameterize a bias correction method to adjust the simulated climate data. Climate bias correction methodologies aim to amend biases or systematic inaccuracies in models by comparing climate model outputs with baseline climate data. The thorough process of climate bias correction methods includes data collection, climate model simulation, bias evaluation, selection of correction techniques, implementation of bias correction, and subsequent assessment and application. Illustration Figure 5 [30].

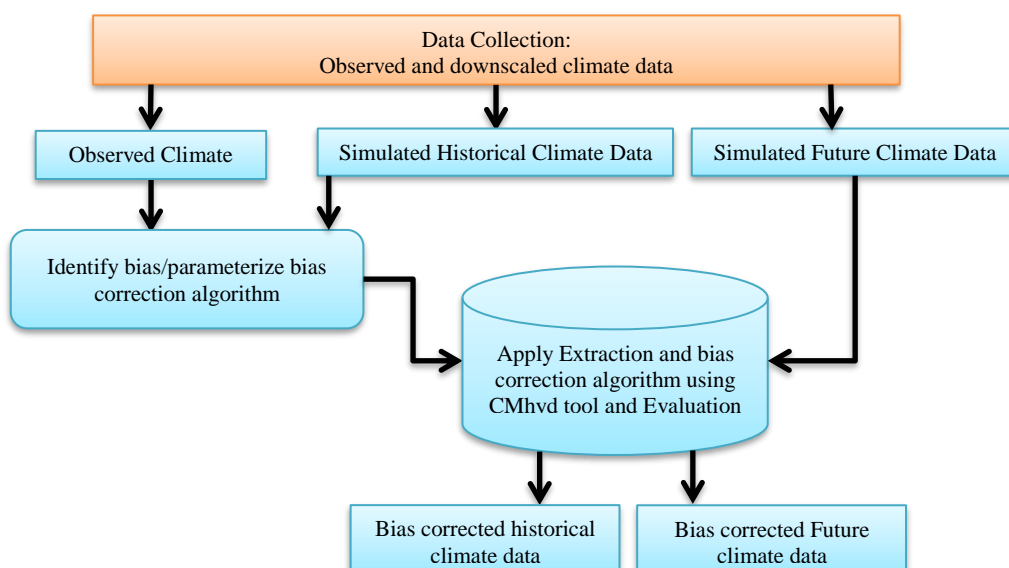


Figure 5. Methodological for rectifying biases in downscaled climate data generated by (GCMs)

3.3. Groundwater Modeling System (GMS)

GMS is a software program designed to perform GW simulations. The software includes a graphical interface and many analysis codes such as MODFLOW 2000, 2005, MODPATH, NT, ART3D, SEAM3D MT3DMS/RT3D, SEEP2D, FEMWATER and UTCHEM. These models are either finite-difference or finite-element models in 2D or 3D. Only models and tools that work with the groundwater model being solved are available for users to select. GMS's strength is its ability to combine a wide range of sub-models in a comprehensive way, as well as its strong GIS preprocessing of a model [31]. GMS enables users to create a groundwater model by spatially defining features and boundaries using vector-based arcs, polygons, and points inside a conceptual model framework. These can represent, for example, wells, aquifers and rivers, which contain specific boundary conditions data, such as pumping rates, material properties and stages. The conceptual models (CMs) are converted into a finite-differences grid by placing the vector elements into the grid. Boundary condition (BC) data is then translated to the respective MODFLOW modules [32]. Groundwater flow in saturated mode is simulated by MODFLOW, which means it does not represent a head value in unsaturated cells, causing them to dry. It was possible to solve the dry cell problem approximately by using several add-on packages for MODFLOW and finding solutions to The Richards equation in one dimension or through the utilization of kinematic wave approximation. Nevertheless, no data was supplied to calibrate the flow within the unsaturated zone [33, 34].

3.4. Quantitative Simulation Models

This study relies on the finite difference numerical method to resolve the governing equations of groundwater flow utilizing the MODFLOW model within GMS software. The model directly interacts with the identical mesh layout. The equation for groundwater flow in an aquifer can be expressed as [35]:

$$\frac{\partial}{\partial x} \left(K_{xx} \frac{\partial h}{\partial x} \right) + \frac{\partial}{\partial y} \left(K_{yy} \frac{\partial h}{\partial y} \right) + \frac{\partial}{\partial z} \left(K_{zz} \frac{\partial h}{\partial z} \right) + W = S_s \frac{\partial h}{\partial t} \quad (3)$$

K_{xx} , K_{yy} , and K_{zz} denote hydraulic conductivities in the XYZ directions (L/T); h represents the potentiometric head (L); W signifies the volumetric flux per unit volume indicating sources and/or sinks of water (T⁻¹); S_s refers to the specific storage of the porous medium (L⁻¹); and t indicates time. Equation 3 applies to groundwater flows in a anisotropic and heterogeneous medium under non-equilibrium conditions. Equation 3 isn't suitable for analytical solutions, so numerical methods must be used. Nevertheless, the equation's solution necessitates knowledge of the heads at the aquifer's boundaries as well as the initial conditions. Various numerical approaches are available, including finite-difference and finite-element methods. The finite-difference approach is utilized in MODFLOW to solve Equation 3 [31].

3.5. Building the Conceptual Model (CM)

To create a CM, it is essential to define the layers, including the outer boundary, sources & sinks, recharge, hydraulic conductivity and observation wells. The most important features for selecting and simplifying the appropriate conceptual model are the level of accuracy required, the objective of problem management, the type of problem being studied (either contaminant or flow), and the intended employed of the model (future forecasting or exploration of the system).

CM is constructed depending on the relevant information collected about the aquifer in the research region. The aquifer is considered a single unconfined aquifer. Data preprocessing and post processing were done using the "map module" within GMS environment. The construction of a MODFLOW simulation in GMS can be achieved through the conceptual model approach and the grid approach.

- The grid approach involves the application of sources and sinks, along with other model parameters, to each cell inside the 3-D grid.
- The conceptual model technique employs GIS technology within the Map module to develop a CM. The spatial coordinates of sources and sinks, layer characteristics such as hydraulic conductivity, model boundaries, and other critical data for simulation can be established at this conceptual model stage. Upon model completion, the grid is established, and the conceptual model is converted into the grid model, with all cell assignments executed automatically.

3.6. Boundary Conditions (BCs)

(BCs) pertain to hydraulic circumstances at the edges of the problem area and can be analytically classified into three types: defined flow boundary, head-dependent boundary, and constant head boundary. The constant-head boundary was implemented on the western and eastern boundaries of the research area. The head values allocated to these boundaries were 5 m and 35 m, respectively. These values were determined based on measurements from observation wells, as depicted in Figure 6. Furthermore, the study area includes two specific features: Tar Al Najaf and Tar Al Sayyed; these are designated as no-flow boundaries at the southwest and northwest edges of the study region.

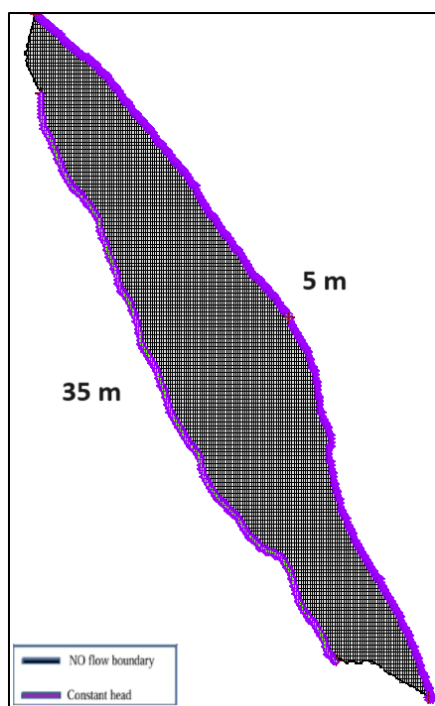


Figure 6. Boundaries of flow model and grid distribution

3.7. Recharge

Recharge significantly influences the behavior and levels of regional groundwater aquifer systems, particularly in dry and semiarid areas, although estimating its quantity is typically difficult [36]. Recharge is an essential factor in groundwater modeling and can be determined using models ranging from simple to complicated. One common approach to determining groundwater recharge rates involves establishing a correlation between precipitation and recharge [37].

Calibrated recharge modeling was utilized due to the difficulty of determining values of field recharge. The spatially calibrated recharge was initially allocated based on an analysis of the water budget and then adjusted until a satisfactory agreement was reached between the observed and calculated groundwater head [27]. The majority of groundwater recharge often happens during rainy seasons like the winter, while some can also occur during those times when there is intermittent rainfall. During periods of low rainfall, particularly in regions with little Precipitation, such as arid and semiarid areas, the recharge impact can be ignored due to insufficient quantity; it must be improved even for soil moisture [36].

3.8. Estimation of Recharge

Accurately calculating recharge is crucial for semiarid and arid regions such as Iraq because these regions mainly rely on precipitation. Recharge can be calculated by the water balance method, which depends on the equality between the output and input, thus, any alteration in the output or input will lead to a corresponding change in storage (ΔS). The groundwater balance can be mathematically represented by the following Equation 4:

$$\Delta S = \text{Input } (P) - \text{Output } (PET + R + \Delta SM) \quad (4)$$

where P represents precipitation (L), PET represents evapotranspiration (L), R represents runoff (L), ΔSM represents a change in soil moisture content (L).

The Thornthwaite method (1948) [38] was employed to calculate accurate potential evaporation. This method is deemed more suitable for the research area than other methods due to its reliance on the average monthly temperature and the adjustment information for available daylight hours. Actual evaporation in this study was estimated using the following five steps:

Step 1. The yearly heat index (I) in degrees Celsius ($^{\circ}\text{C}$) can be calculated employing the following formula:

$$I = \sum_{i=1}^{12} \left(\frac{T_i}{5} \right)^{1.514} \quad (5)$$

where T_i denotes the average monthly temperature measured in degrees Celsius ($^{\circ}\text{C}$).

Step 2. Applying the following formula to calculate the constant (a):

$$a = 0.016I + 0.5 \quad (6)$$

Step 3. Utilizing the corrected factor table to estimate the daylight correction factor (K), this is dependent on latitude and geographic location [38].

Step 4. Finally, apply the following formula to determine the corrected monthly potential evapotranspiration (PE_c):

$$PE_c = K \times 16 \times \left(\frac{10T_i}{I}\right)^a \quad (7)$$

The final potential evapotranspiration estimates directly from Table 2 for mean monthly temperatures equal to or exceeding 26.5 °C, but these steps are employed for mean monthly temperatures less than or equal to 26.5 °C.

The following criteria are utilized in determining actual evapotranspiration after potential evapotranspiration has been calculated [21]:

$$IF: R > PE_c \quad Then \quad AE = PE_c \quad (8)$$

$$IF: R < PE_c \quad Then \quad AE = R \quad (9)$$

R denotes the annual rainfall depth, (PE_c) denotes the corrected potential evaporation, and AE denotes the actual evapotranspiration.

The necessary soil moisture data for this research region were obtained from the European Centre for Medium-Range Weather Forecasts (ECMWF) website at <https://www.ecmwf.int/>. ΔSM is determined by subtracting the previous month's value from the next month's value. The equation provided can be used to compute the values of excess water.

$$WS = R - (AE + \Delta SM) \quad (10)$$

where ΔSM represents the change in soil moisture, WS represents water surplus.

The (SCS) method was employed to estimate runoff values from precipitation in Iraqi governorates due to the scarcity of information. The General Commission of Groundwater reports that there are 500 to 600 operational wells in the research area. Typically, the depths of the wells varied from 20 to 90 meters, and the pumping rates ranged from 25 to 30 cubic meters per hour. The wells had a specified capacity ranging from 5 to 220 cubic meters per hour [26]. The value of the total abstraction rate could be computed as follows using the average well operation times and the withdrawal rates of the pumps:

$$Total \ withdrawal = (pumping \ rate \times operation \ time \times days \ operation/year) \times number \ of \ production \ wells/365$$

Assuming the operation period is between six to eight hours per day, with an average discharge rate of eight liters per second and operating for 145 days per year, the yearly pumping rate is 11,000 cubic meters per day. The computed values were input for the simulation model because no direct field observations were available.

4. Results and Discussion

4.1. Calibration and Validation of Temperature and Precipitation

This study utilized temperature and rainfall data to calibrate and confirm the outcomes of climate model simulations after applying bias corrections. The data gathered at each site were employed to calibrate and validate the model. The dataset was partitioned into two segments: data from 1983 to 2014 was utilized for calibration, while data from 2015 to 2022 was allocated for the validation of each predictor. Statistical criteria were utilized to evaluate the efficacy of climate models and bias correction techniques. Mustafa & Mawlood [35] utilized four model evaluation methods to evaluate the effectiveness of chosen RCM models and bias correction techniques: (R^2), (PBIAS), (NSE), and (RMSE).

RMSE was a goodness-of-fit indicator indicating the standard deviation between predicted and actual data. Model performance enhances as RMSE diminishes. Furthermore, the goodness of fit between the predicted and observed data was assessed using R^2 , indicating that the model's performance improved as R^2 neared one. The NSE ranges from negative infinity to 1; Moriasi et al. [39] established that an NSE value of 1 indicates optimal reliability, values between 0.6 and 0.8 represent medium to good dependability, and values over 0.8 are considered extremely good. PBIAS measures the mean divergence of simulated data from empirical values. The generated dataset surpasses the actual dataset for negative values, signifying overestimation, while it is inferior to the observed dataset for positive values. The ideal value of PBIAS is 0.0. A PBIAS value of ± 5 is frequently regarded as an acceptable margin of error for the mode. The results of calibration and validation are presented in Tables 4 and 5.

Table 4. Indicators of the statistical effectiveness of bias correction methods for precipitation and temperature

Station	Variable	Performance Indicators	SSP2-4.5	SSP5-8.5
Karbala	Precipitation	R ²	0.982	0.995
		RMSE	3.547	2.064
		NSE	0.634	0.876
		Pbias	-0.298	-0.205
Najaf		R ²	0.984	0.986
		RMSE	3.403	2.628
		NSE	0.699	0.821
		Pbias	-0.307	-0.231
Temperature				
Karbala	Maximum Temperature	R ²	0.999	0.999
		RMSE	2.493	2.872
		NSE	0.945	0.927
		Pbias	-0.072	-0.084
Najaf		R ²	0.998	0.997
		RMSE	2.493	2.829
		NSE	0.924	0.904
		Pbias	-0.142	-0.163
Karbala	Minimum Temperature	R ²	0.998	0.997
		RMSE	2.579	2.982
		NSE	0.982	0.894
		Pbias	-0.142	-0.163
Najaf		R ²	0.999	0.999
		RMSE	2.533	3.026
		NSE	0.943	0.918
		Pbias	-0.073	-0.086

Table 5. Statistical indicators for model validation for precipitation and temperatures

Station name	Statistics	PCP	T _{max}	T _{min}
Karbala	R ²	0.954	0.999	0.999
	RMSE	3.111	0.916	0.783
	P-BIAS	0.035	0.023	0.036
	NSE	0.814	0.993	0.993
Najaf	R ²	0.954	0.999	0.999
	RMSE	3.484	0.944	0.857
	P-BIAS	-0.104	0.024	0.040
	NSE	0.807	0.992	0.991

4.2. Climate Change Scenarios

The IPCC provided climate change scenarios as a ratio of precipitation and air temperature between future periods and a baseline period. The near future is defined as the period from 2023 to 2050, using a baseline period of 1983 to 2022. GCMs are frequently employed to evaluate the influences of climate change on water resources. GCMs forecasted that the climate of the research area would experience significantly increased temperature and rainfall compared to the historical period, 1983–2022. The ACCESS - CM2 and BCC - CSM2 -MR climate models project an increase in mean annual rainfall over baseline conditions by approximately 1.9 mm/year and 1.3 mm/year, respectively, from 2023 to 2050, resulting in mean annual precipitation values of 8.35 mm and 7.75 mm, respectively.

Conversely, the MIROC6 model projected the mean annual precipitation would be considerably lower than the baseline condition by around -0.5 mm/year. The average yearly precipitation decreased to 5.97 mm for Karbala station, as shown in Figure 8. Additionally, the ACCESS - CM2, BCC - CSM2 -MR, and MIROC6 climate models projected that the mean annual precipitation will increase above baseline conditions by around 2, 0.5, and 0.4 mm/year, respectively, from 2023 to 2050, as shown in Figure 7.

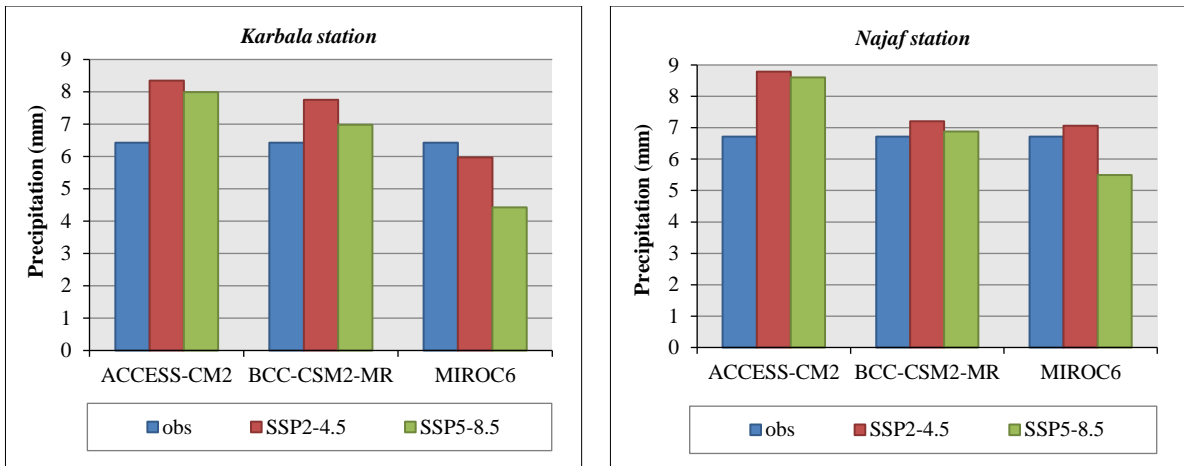


Figure 7. A contrast of the expected values to the recorded mean monthly precipitation

The anticipated mean annual temperature increases are 2.4(2.4), 2.4(1.6), and 1.7(0.3)°C for the ACCESS -CM2, BCC -CSM2-MR, and MIROC6 models with the SSP2 –4.5 scenario for the Karbala (Najaf) station, respectively. Under the SSP5–8.5 scenario, the increases are expected to be 2.5(2.4), 2.7(2), and 1.8(0.5) °C for the same models at the same station during the period from 2023 to 2050. In this research, the adopted scenarios were from the Sixth Assessment Report. The aim is to analyze the influence of climate change on groundwater recharge between 2025 and 2035, as shown in Figure 8.

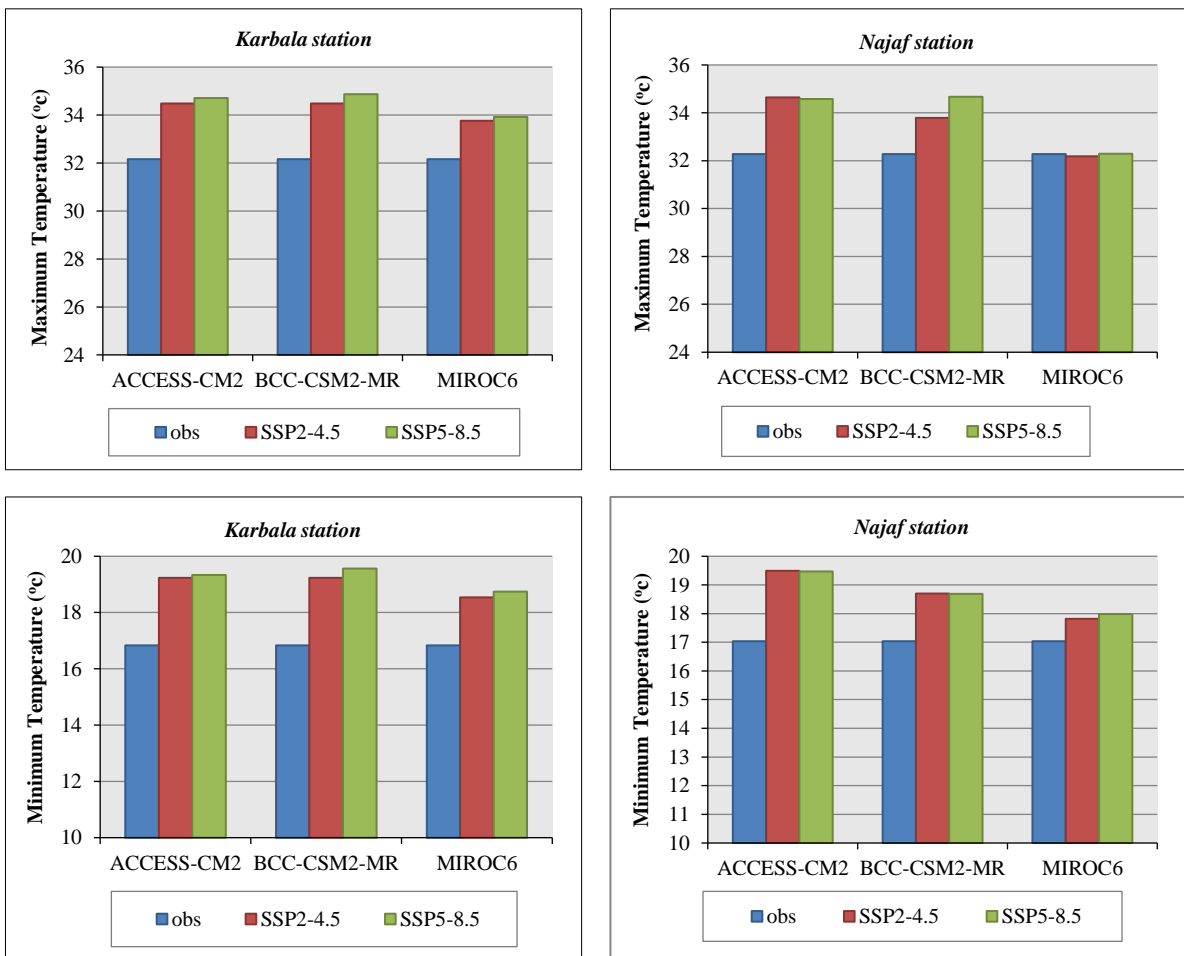


Figure 8. A comparison of the anticipated values to the observed average monthly temperature

Figures 9 and 10 illustrate the mean yearly precipitation of ensemble (GCMs) for 2023–2035 under ACCESS -CM2 climate model for the SSP2 –4.5 scenario.

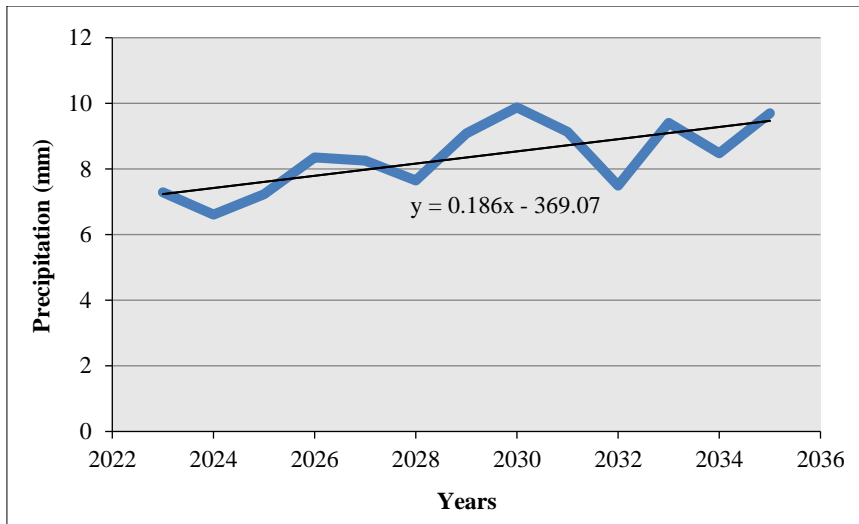


Figure 9. Annual precipitation for Karbala station for the period 2022–2035

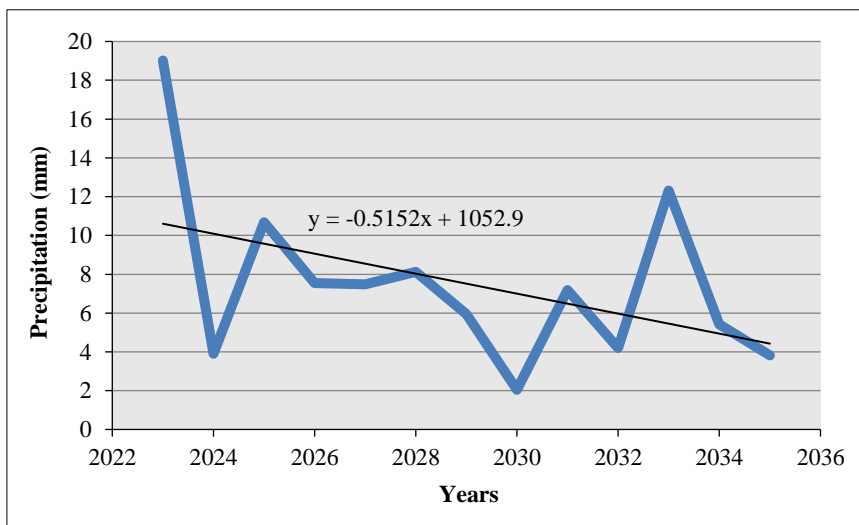


Figure 10. Annual precipitation for Najaf station for the period 2022–2035

The climate diagrams display monthly averages for rainfall and temperature over a year. Climate diagram for Karbala and Najaf stations confirms the characteristics of weather conditions were in the "extreme" category. According to the Walter–Laeth climate diagram, drought prevailed for almost months. The wet period occurred in December, November, January and February, as shown in Figures 11 and 12.

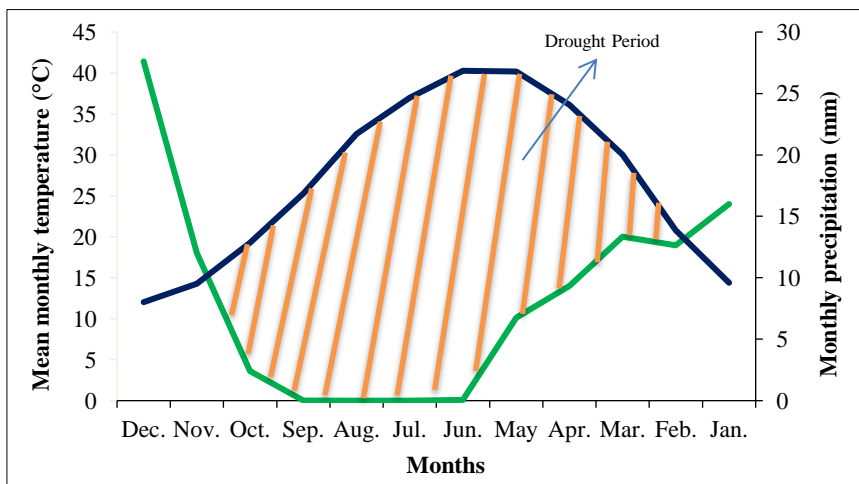


Figure 11. Climate diagram for Karbala station for the period 2022–2035 (* Temperature trends are displayed as a blue line and precipitation trends are displayed as a green line).

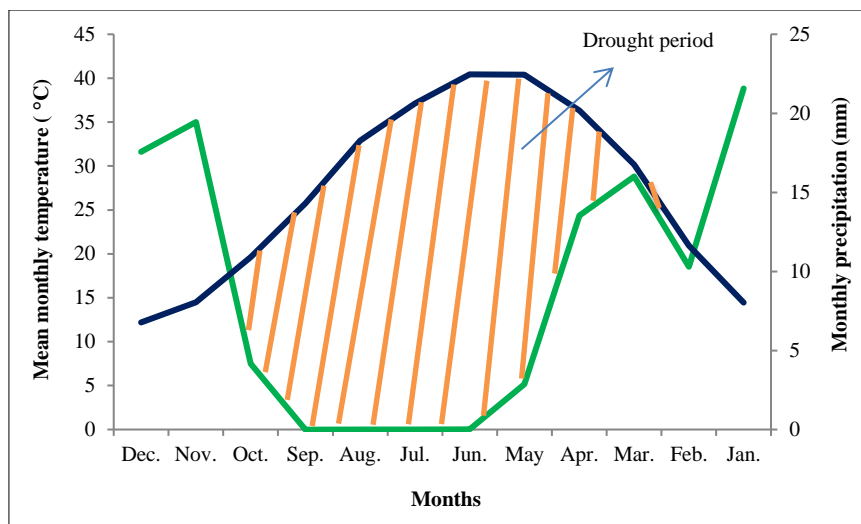


Figure 12. Climate diagram for Najaf station for the period 2022–2035 (* Temperature trends are displayed as a blue line and precipitation trends are displayed as a green line).

4.3. Model Calibration in Steady State

The developed model needs to show a better fit between observed and simulated values before it can be used for prediction. For the model, calibrations in steady state and transient states were done. While the transient calibration was performed employing measurements of groundwater head for (4) wells, the calibration in steady-state was performed using the groundwater head data for (7) wells. These seven wells were chosen to represent the entire study area and reduce the simulation runtime during the calibration process, which was conducted automatically utilizing PEST tools (parameter estimation) in the GMS. The calibrated steady state is essential for the transient state as it signifies the initial condition of transient models. Calibration can be performed manually or automatically through an optimization approach known as PEST. Adjusting the input variables is required to match the measured and simulated heads best. Hydraulic conductivity is the most crucial characteristic compared to the other components. The simulated heads proved acceptable if the discrepancy between the actual and simulated heads was equal to or less than ± 0.5 m. The modified input variables were recharge rates and hydraulic conductivities. Table 6 compares the simulated and observed head values.

Table 6. Comparison between simulated and observed head

No. well	X(UTM)	Y(UTM)	Observed Head	Observed Head Interval	Observed Head Confidence (%)	Simulated Head	Residual Head
W1	413578.0	3599681.0	17.3	0.5	95	16.91298	0.38702
W2	421538.0	3576704.0	19.0	0.5	95	18.93862	0.06138
W3	425307.0	3577168.0	15.5	0.5	95	15.3185	0.1815
W4	433377.0	3559898.0	11.0	0.5	95	11.50768	-0.50768
W5	432260.0	3553378.0	21.0	0.5	95	20.808	0.192
W6	412131.0	3603145.0	14.0	0.5	95	13.99679	0.00321
W7	404127.0	3605170.0	26.5	0.5	95	26.94971	-0.44971

The MODFLOW/ PEST module has been run to estimate the parameters hydraulic conductivity and recharge rates as given in Table 7.

Table 7. Parameter estimation results

Parameter keys	Initial value m/day	Estimated value m/day
HK_10	17.5	18.194
HK_20	12.5	5.56084
HK_30	7.5	1.05776
HK_40	2.5	20
RH_100	0.000822	0.000001

Figure 13 illustrates a contour map of the observed heads for the aquifer after calibration. In the steady state calibration, six of the seven observation targets are indicated by green error bars. Only one error bar was yellow; however, they were within the target's allowable limit, significantly improving the initial solution.

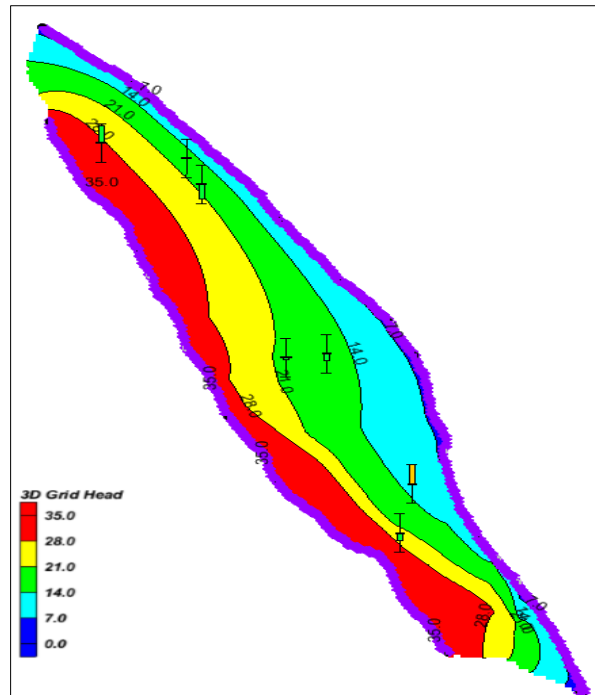


Figure 13. Contour map of simulated heads after calibration of Dibdiba aquifer

Several techniques are used to evaluate the calibration process, regardless of whether it is done manually (trial and error) or automatically. The most widely used method is to compute the residuals, or difference between simulated and measured heads, which may be compared statistically or graphically to help quantify the calibration process. By comparing the calibrated model with the acceptable threshold values, the minimum residual value and standard deviation should be obtained. The model calibration process is typically evaluated using standard statistics such as mean error (ME), mean absolute error (MAE), root mean square error (RMSE), and mean relative error (MRE), as shown in the table. The equations utilized for these statistics are presented here:

$$ME = \frac{1}{n} (\sum_{i=1}^n O_i - S_i) \tag{11}$$

$$MAE = \frac{1}{n} (\sum_{i=1}^n |O_i - S_i|) \tag{12}$$

$$RMSE = \sqrt{\frac{\sum_{i=1}^n (O_i - S_i)^2}{n}} \tag{13}$$

$$MRE = \frac{RMSE}{\Delta} \tag{14}$$

S_i and O_i represent the simulated and observed data at the observation well i . The MRE is the difference between the maximum and minimum observed values, denoted by Δ . ME between observed and simulated heads, ideally zero for the aquifers, was nearly zero (-0.0189) as shown in Table 8. MAE, MRE and RMSE were low, which illustrates that the groundwater flow can be predicted using BC, CM and final hydrological, reliable parameters.

Table 8. Summary of steady state calibration error

Evaluation Criteria	Error value
ME	-0.0189
MAE	0.254643
RMSE	0.312444
MRE	0.020158

Figure 14 shows the correlation between the simulated and measured water levels. The determination coefficient (R^2) was calculated to be 0.9956, showing a strong correlation between the measured and simulated and values.

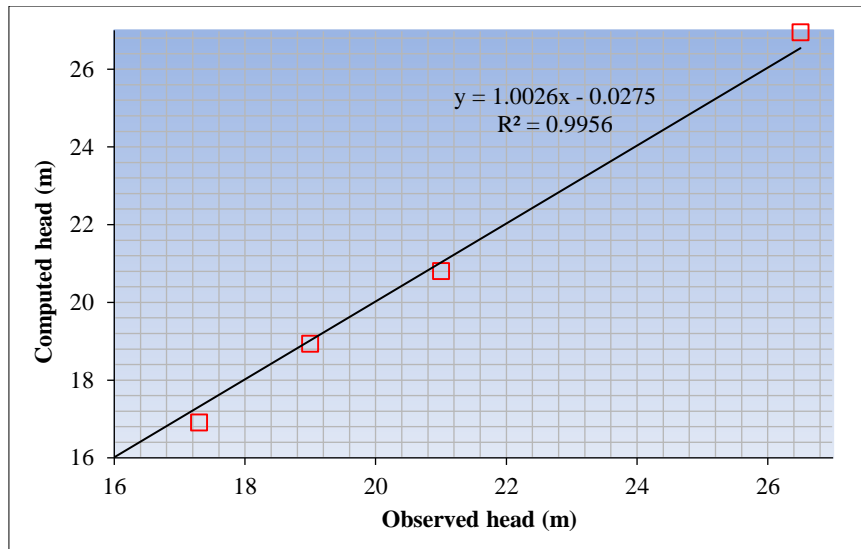


Figure 14. Scatter plot of computed vs. observed head

4.4. Model Calibration in Transient State

An accurate assessment of recharge rates and hydraulic conductivities derived from the steady state condition is essential for successful transient calibration. The corresponding observed groundwater heads from four wells were among the data employed for the calibration and validation processes (Figure 1). Since the study's findings will be focused on the area near the Karbala WWTP, the positions of these wells approximately represent the area.

For transient state calibration, a new parameter called "specific yield" was created and adjusted during the transition calibration until a good agreement was achieved between the simulated and measured heads in the simulation period (July 2023 to April 2024). During the calibration of the transient state, values of specific yield were adjusted by a trial and error method until a satisfactory match between the simulated and observed heads was reached Figure 15.

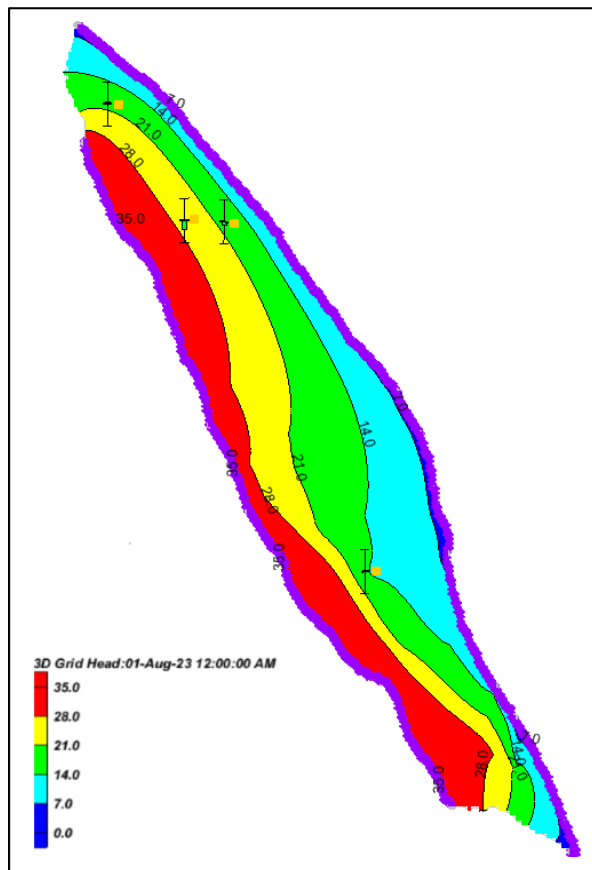


Figure 15. Contour map of the simulated aquifer water heads in Sep 2023

The model displays four calibration targets distinguished by the color green. The transient model was evaluated employing a transient scatter plot of observed data against computed aquifer heads, as illustrated in (Figure 16). The scatter plot shows a determination coefficient $R^2 = 0.9993$.

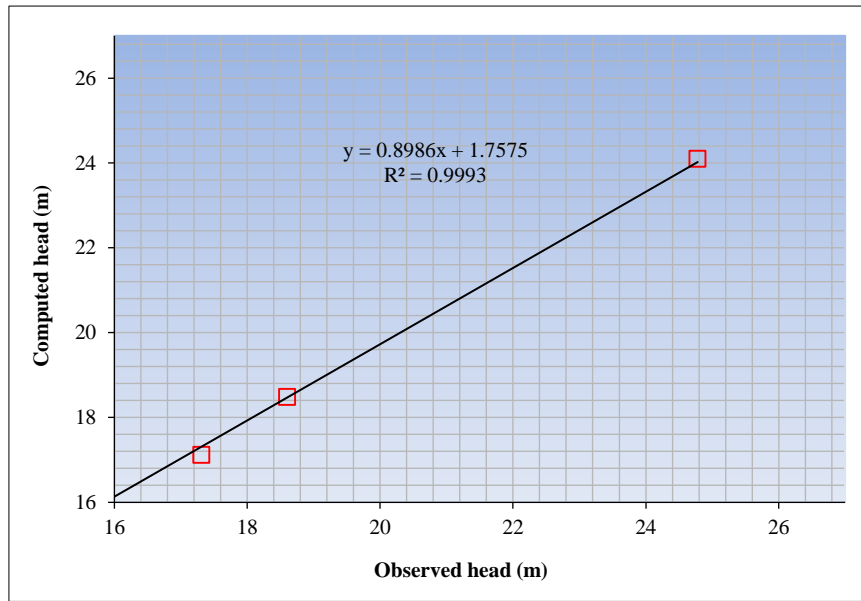


Figure 16. Scatter plot of computed vs. observed head for transient simulation at Sep 2023

The groundwater flow model was validated employing the (MAE) and (RMSE) over the stress period. The findings are presented in Table 9. The RMSE fluctuates across most periods and remains below 1 meter, confirming the simulation's dependability

Table 9. Transient state calibration error

Assessment Criteria	Error value
ME	-0.15
MAE	0.61
RMSE	0.86

Figure 17 presents a time series plot of transient observation wells data, illustrating the correlation between computed and observed periodic head values. The model demonstrated excellent results during the transient simulation. The calibrated model can be utilized to forecast groundwater levels.

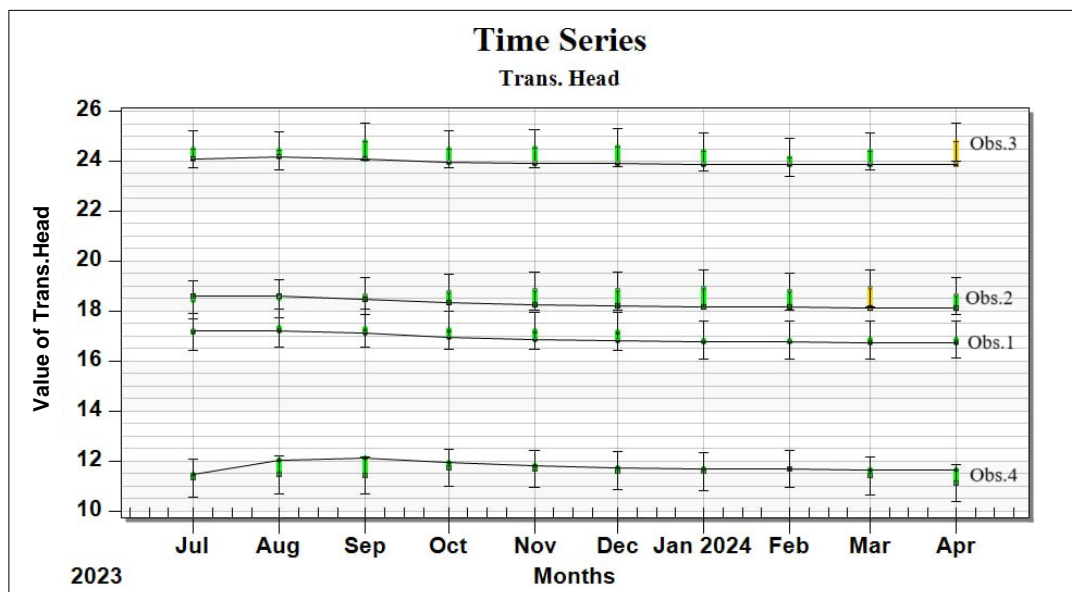


Figure 17. Time series plot for transient observation wells

4.5. Sensitivity Analysis of the Parameters

Parameter sensitivity is an effective method for evaluating the influence of each parameter and distinguishing between large, minor, and negligible effects of these parameters on the model's expected outcomes. It helps to assess the importance of parameters in determining which data should be provided with high accuracy and which data must be provided with low accuracy. Therefore, the sensitivity of the analysis helps to decide the most critical parameter affecting the last results [40]. A sensitivity analysis was conducted after calibration with PEST at both steady and transient states. RCH and HK of the steady-state parameters. The transient state sensitivity analysis parameter was specific storage. Figure 18 shows the sensitivity analysis obtained via plot wizard in GMS for steady state.

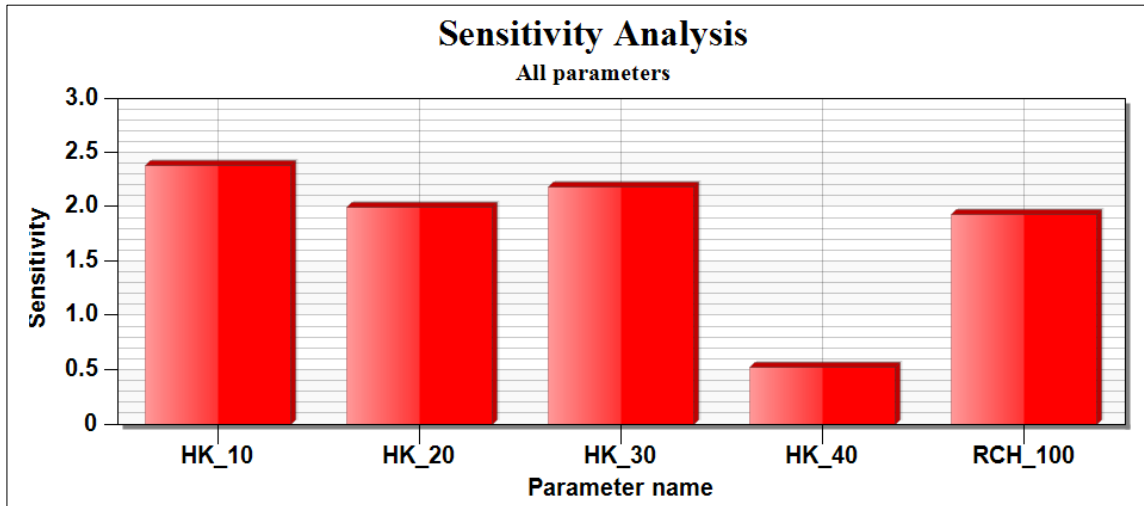


Figure 18. Sensitivity analysis of steady state model

It is evident from the sensitivity analysis that hydraulic conductivity is the most effective on the groundwater in this system. The symbols HK -10, HK -20, HK -30 and HK -40 are used in the GMS program to refer to the hydraulic conductivity of each stratum. RCH-100 is the symbol that leads to the recharging rate.

The data presented in Figure 19 can be employed to differentiate between the parameters significantly influencing the model's outcomes and those with minimal impact. The parameter identified as code (SY_20) substantially impacts the model's outcomes relative to other employed parameters, indicating that the model exhibits sensitivity to variations in specific storage within the SY_20 zone.

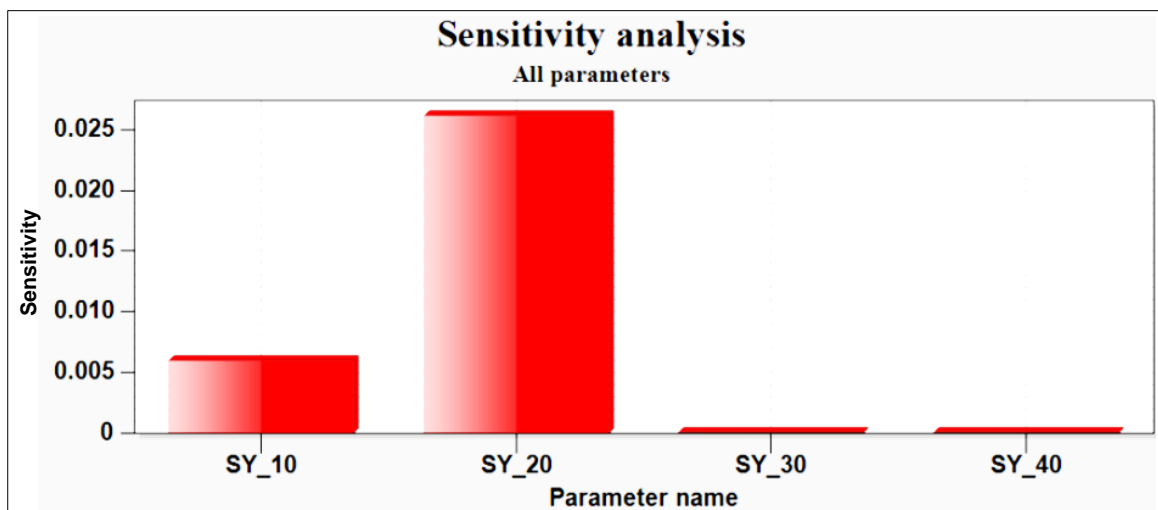


Figure 19. Sensitivity analysis of transient model

4.6. Effect of Climate Change and Artificial Recharge on Groundwater Replenishment

Variations in precipitation regime and quantity and changes in evapotranspiration and temperature impact groundwater recharging. In general, groundwater recharging will increase in regions that witness increased precipitation and vice versa. Groundwater recharge will also increase in regions where permafrost thaws. Groundwater recharge also increases significantly during the cold months as more infiltration into the soil. Evapotranspiration rates in the research region increase throughout the hot months due to rising temperatures and increased water availability.

Artificial recharge is a promising adaptation measure to reduce the effect of global warming. It plays an important role in restoring the groundwater balance and as a measure to control over-abstraction. Estimates of forecasted groundwater levels from the calibrated groundwater model covering the whole research region were employed to determine possible climate change effects on GW storage, focusing on the area surrounding the Kerbala WWTP. For this, three GCMs (ACCESS-CM2, BCC-CSM2-MR, and MIROC6) with SSP 2-4.5 and SSP 5-8.5 scenarios were considered. The temperature and rainfall data from GCMs were retrieved and employed in mudflow to predict the groundwater levels. Table 8 displays the amount of current and projected recharge in the future. The forecasted recharge rises by 22% in comparison to the present recharge for the research region. This increase could be due to an increase in precipitation. Table 10 indicates that more water is recharged to the aquifer under SSP 2- 4.5 relative to current conditions. However, more than this recharge is needed to compensate for the decrease in groundwater levels resulting from excessive withdrawal.

Table 10. Current recharge and projected recharge under SSP2-4.5 of near future

Conditions	Recharge (mm/year)
Current conditions	22.82
SSP2-4.5 scenario	27.98

Several scenarios were developed to overview the influence of global warming and artificial recharge of groundwater of the research region under different scenarios and summarized as follows, focusing on the area surrounding the Kerbala WWTP.

4.6.1. First Scenario: Natural Recharge under SSP2-4.5 for ACCESS-CM2 Model

The major component of the groundwater recharge is precipitation. The region receives an annual precipitation of (103) mm from 2025 to 2035 at Karbala and Najaf stations. The natural recharge is estimated (27.98) mm/year. In this scenario, the natural recharge and the present extraction (11000 m³/d) were used to protect the groundwater levels, which were used as reference levels to compare with other scenarios. Figure 20 shows the projected hydraulic head depend on a 10-year modeling period from 2025 to 2035 in 20 pumping wells within the simulated region. The largest rise in the head, relative to observed values, exceeded 0.5 m in four of the observation wells. The rise in the head is projected to be between 0.45 and 0.7 meters by 2035 compared to the present head level.

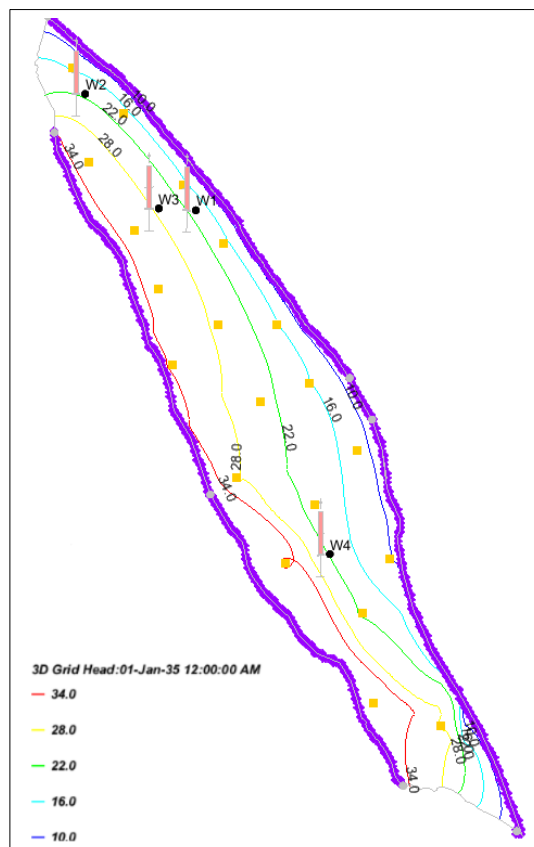


Figure 20. Heads of groundwater after increasing recharge by adding 10%.treated wastewater

4.6.2. Second Scenario: Natural Recharge under SSP2-4.5 and 10% Artificial Recharge

The groundwater level is affected by recharge volumes, which mainly depend on precipitation intensity. In this scenario, SSP2-4.5 under the ACCESS-CM2 model anticipated an increase in Tmax by about 3.4°C and an increase in precipitation by about 2mm shortly. This alteration in climate data was implemented in the aquifer to calculate the groundwater recharge. The groundwater recharge was augmented by adding 10% of the wastewater treatment plant effluent (6,000 m³/day) as an artificial recharge to study the influence of this increase on the investigation region. Figure 21 shows the anticipated hydraulic head. Compared with measured values, the maximum increase in the head exceeded (1) m in four of the observation wells. The forecasted rise in head is estimated to range from 0.4 to 1.1 meters by 2035 compared to the current head level.

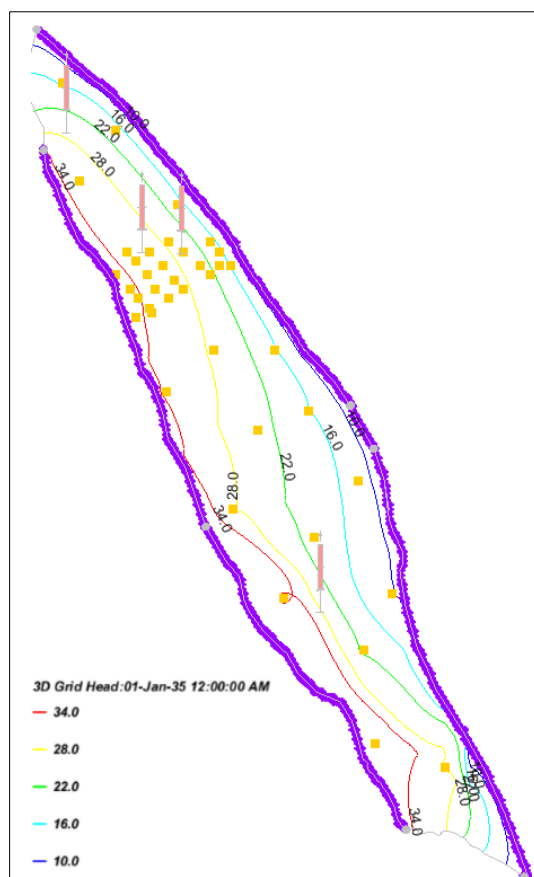


Figure 21. Heads of groundwater after increasing recharge by adding 10%.treated wastewater

4.6.3. Third Scenario: Natural Recharge under SSP2-4.5 and 15% Artificial Recharge

This scenario will investigate the result of increasing the natural recharge by adding 15% of the wastewater treatment plant outflow (9,000 m³/day) employed as artificial recharge to evaluate the effect on the research region that may result from these increments. In this scenario, SSP2-4.5 under the ACCESS-CM2 model projected a rise in maximum temperature of around 3.4°C and an increase in precipitation of around 2 mm shortly. This change in climate data was employed to determine the groundwater recharge in the aquifer. The natural recharge is estimated at 27.98 mm/year. Figure 22 shows the anticipated hydraulic head. The rate of increase in groundwater levels for this scenario is 1.75 m, where the lowest increase in well 3 is (1.15) m, and the highest increase in well 1 is (1.75) m.

4.6.4. Fourth Scenario: Natural Recharge under SSP2-4.5 and 20% Artificial Recharge

In the fourth scenario, illustrated in Figure 24, the natural recharge remained the same as in the second and third scenarios, whereas the artificial recharge rate increased to 20% of the WWTP outflow (12,000 m³/day). Under this scenario, the groundwater level increase can be shown. Figure 23 shows the anticipated hydraulic head. When compared with measured values, the largest increase in the head exceeded 1.5 meters in four of the observation wells. The rise in the head reaches between (0.4 to 1.95 m) in 2035 when compared to the present head. Applying this scenario up to 2035 would provide an opportunity to manage groundwater sources in the future effectively.

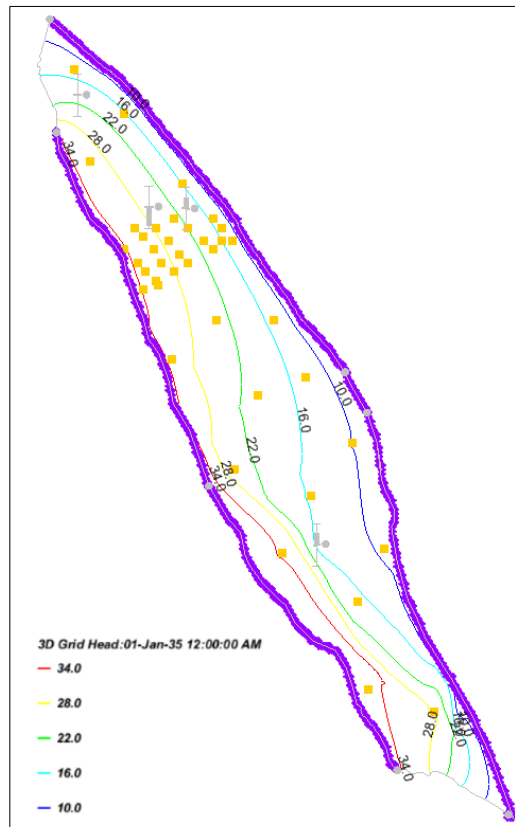


Figure 22. Heads of groundwater after increasing recharge by adding 15% treated wastewater

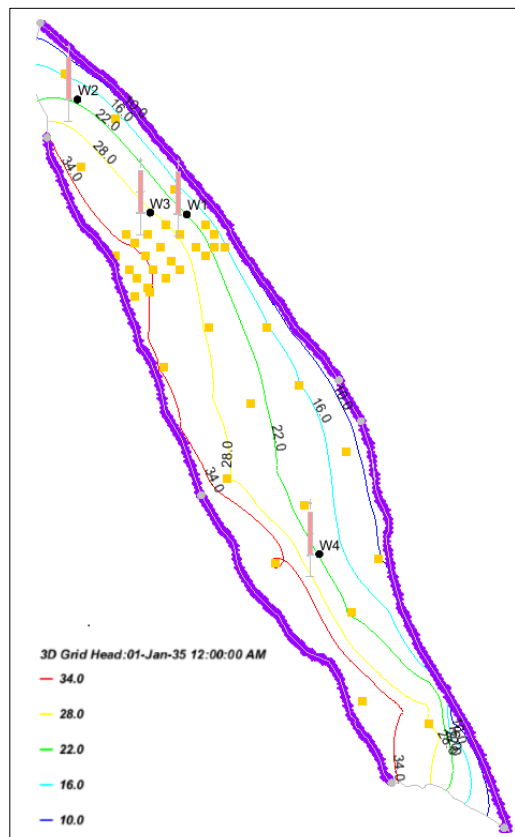


Figure 23. Heads of groundwater after increasing recharge by adding 20% treated wastewater

The last three scenarios implemented artificial recharge in twenty chosen wells. These recharge wells were located near WWTP for operational and economic reasons. The aquifer response illustrated that during the predicted period (2025 to 2035), the application of artificial recharge would raise the groundwater level in (Obs1 and Obs3) by about 1 and 0.8 m for the second scenario with a pumping rate for artificial recharge of 6000 m³/day. In (Obs2), the increment

in groundwater level is about 0.4 cm. The comparison of the simulated groundwater head for 2035 depended on the first and second scenarios, a maximum rise of approximately 1.5 meters might be obtained by using a pumping rate for artificial recharge of 6000 m³/day and based on the first and third scenarios indicated that the maximum increase of approximately 1.85 m might be achieved by using a pumping rate for artificial recharge of 9000 m³/day. The results of the rising groundwater levels align with prior studies.

On the other hand, the increment in groundwater level based on the first and third scenarios indicated that the maximum increase of approximately 2.25 m might be achieved by using a pumping rate for artificial recharge of 12000 m³/day. These results indicate that using artificial recharge wells in recharge wells will improve the groundwater level, as shown in Figures 24 to 27. Induced water impact decreases further away from artificial recharge wells. The result of the study showed that artificial recharge will have significant impact on groundwater at aquifer causing increase in groundwater storage and accordingly a considerable rise in groundwater table.

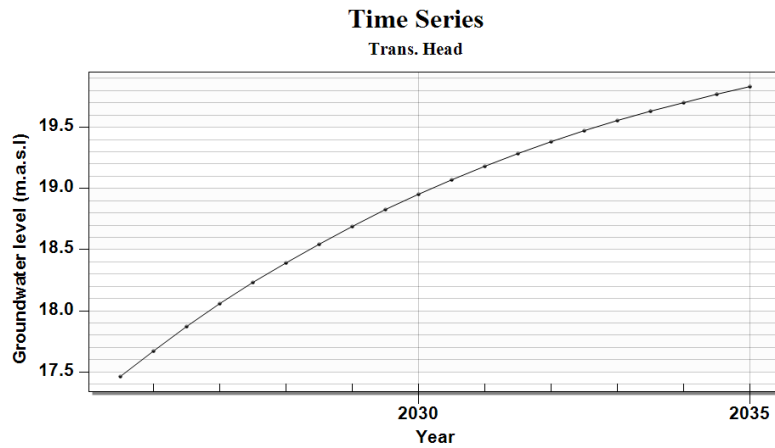


Figure 24. Variations in Groundwater level at observation well No.1 (Obs.1) under SSP2-4.5 scenario for period (Jan. 2025 to Dec. 2035)

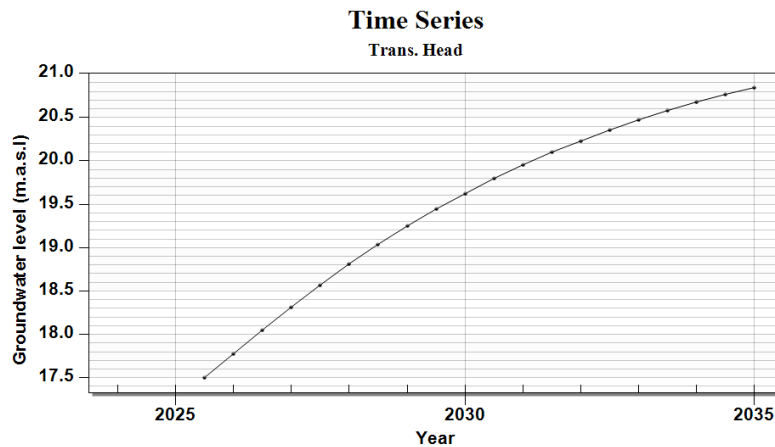


Figure 25. Variations in groundwater level at observation well No.1 (Obs.1) under SSP2-4.5 scenario and 10% artificial recharge for period (Jan. 2025 to Dec. 2035)

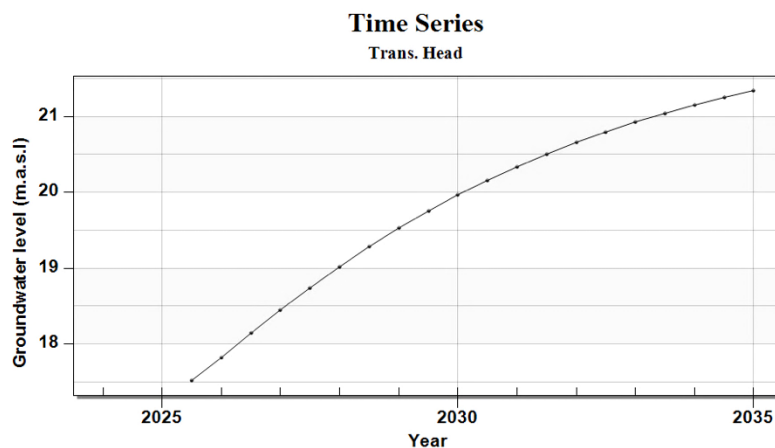


Figure 26. Variations in groundwater level at observation well No.1 (Obs.1) under SSP2-4.5 scenario and 15% artificial recharge for period (Jan. 2025 to Dec. 2035)

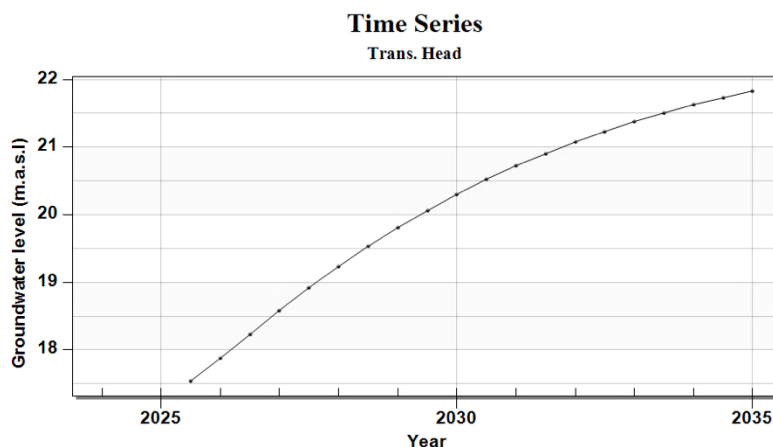


Figure 27. Variations in groundwater level at observation well No.1 (Obs.1) under SSP2-4.5 and 20% artificial recharge for period (Jan. 2025 to Dec. 2035)

5. Conclusions

Groundwater has a vital role in worldwide freshwater sources and is very susceptible to variability and climate change impacts. A proper comprehension of the potential influences of variability and global warming on groundwater resource sustainability and availability. Understanding variability and climatic change is crucial for the management of aquifer resources. Thus, there is a need to assess and comprehend long-term variability and climate change. The influence of climate change and artificial recharge on groundwater levels was studied using the groundwater flow model (MODFLOW). Three GCMs (ACCESS-CM2, BCC-CSM2-MR, and MIROC6) with two SSPs (4.5 and 8.5) were chosen from several GCMs and downscaled by the CMhyd to forecast future precipitation and temperature near the future (2022–2050) periods that were employed for forecasting in the aquifer. The application of artificial recharge of the shallow aquifer in the research region is a significant tool for maintaining groundwater levels. The findings show that the mean yearly precipitation in the research region will increase by about 2mm, while the average yearly maximum temperature will increase by about 3.4°C under SSP2-4.5. Numerical simulations were performed to explore the feasibility of implementing artificial recharge devices. The calibrated models were utilized to simulate four distinct scenarios. One scenario entailed implementing natural recharge under SSP 2-4.5 for the ACCESS-CM2 model without artificial recharge, while three scenarios used artificial recharge via 20 designated wells (6000, 9000, and 12000 m³/day) to demonstrate the aquifer's response throughout the future period of 2025–2035. The modeling findings showed that the increment in groundwater level is about 1, 1.85, and 2.25 m with artificial recharge of about 6000 m³/day, 9000 m³/day, and 12000 m³/day, respectively. According to the findings of this study, artificial recharge using treated wastewater is an interesting climate change mitigation technique.

6. Declarations

6.1. Author Contributions

Conceptualization, W.H.; methodology, W.H. and R.M.; software, R.M.; validation, W.H., R.M., and S.A.; formal analysis, R.M.; investigation, S.K.; resources, W.H.; data curation, R.M.; writing—original draft preparation, R.M.; writing—review and editing, W.H.; visualization, R.M.; supervision, S.K.; project administration, W.H.; funding acquisition, R.M. All authors have read and agreed to the published version of the manuscript.

6.2. Data Availability Statement

The data presented in this study are available on request from the corresponding author.

6.3. Funding

The authors received no financial support for the research, authorship, and/or publication of this article.

6.4. Conflicts of Interest

The authors declare no conflict of interest.

7. References

- [1] Al-Qurnawy, L. S., Almallah, I. A., & Alrubaye, A. (2024). Hydrochemical Characteristics and Spatial Variability in Coastal Aquifers Southern Iraq Utilizing a GIS Technique. *Iraqi Geological Journal*, 57(2), 264–276. doi:10.46717/igj.57.2C.18ms-2024-9-26.
- [2] Hassan, W. H., & Khalaf, R. M. (2020). Optimum Groundwater use Management Models by Genetic Algorithms in Karbala Desert, Iraq. *IOP Conference Series: Materials Science and Engineering*, 928(2), 22141. doi:10.1088/1757-899X/928/2/022141.

- [3] Mohammed, Z. M., & Hassan, W. H. (2022). Climate change and the projection of future temperature and precipitation in southern Iraq using a LARS-WG model. *Modeling Earth Systems and Environment*, 8(3), 4205–4218. doi:10.1007/s40808-022-01358-x.
- [4] Kløve, B., Ala-Aho, P., Bertrand, G., Gurdak, J. J., Kupfersberger, H., Kværner, J., Muotka, T., Mykrä, H., Preda, E., Rossi, P., Uvo, C. B., Velasco, E., & Pulido-Velazquez, M. (2014). Climate change impacts on groundwater and dependent ecosystems. *Journal of Hydrology*, 518(PB), 250–266. doi:10.1016/j.jhydrol.2013.06.037.
- [5] Asadi, R., Zamaniannejatzadeh, M., & Eilbeigy, M. (2023). Assessing the Impact of Human Activities and Climate Change Effects on Groundwater Quantity and Quality: A Case Study of the Western Varamin Plain, Iran. *Water (Switzerland)*, 15(18), 3196. doi:10.3390/w15183196.
- [6] Hassan, W., Faisal, A., Abed, E., Al-Ansari, N., & Saleh, B. (2021). New composite sorbent for removal of sulfate ions from simulated and real groundwater in the batch and continuous tests. *Molecules*, 26(14), 4356. doi:10.3390/molecules26144356.
- [7] Mohsen, K. A., Nile, B. K., & Hassan, W. H. (2020). Experimental work on improving the efficiency of storm networks using a new galley design filter bucket. *IOP Conference Series: Materials Science and Engineering*, 671(1), 12094. doi:10.1088/1757-899X/671/1/012094.
- [8] Aladejana, J. A., Kalin, R. M., Sentenac, P., & Hassan, I. (2020). Assessing the impact of climate change on groundwater quality of the shallow coastal aquifer of eastern dahomey basin, Southwestern Nigeria. *Water (Switzerland)*, 12(1), 224. doi:10.3390/w12010224.
- [9] Treidel, H., Martin-Bordes, J. L., & Gurdak, J. J. (2011). *Climate Change Effects on Groundwater Resources*. CRC Press, London, United Kingdom. doi:10.1201/b11611.
- [10] Sajjad, M. M., Wang, J., Abbas, H., Ullah, I., Khan, R., & Ali, F. (2022). Impact of Climate and Land-Use Change on Groundwater Resources, Study of Faisalabad District, Pakistan. *Atmosphere*, 13(7), 1097. doi:10.3390/atmos13071097.
- [11] Hassan, W. H., & Hashim, F. S. (2021). Studying the impact of climate change on the average temperature using CanESM2 and HadCM3 modelling in Iraq. *International Journal of Global Warming*, 24(2), 131–148. doi:10.1504/IJGW.2021.115898.
- [12] Munday, P. L., Donelson, J. M., & Domingos, J. A. (2017). Potential for adaptation to climate change in a coral reef fish. *Global Change Biology*, 23(1), 307–317. doi:10.1111/gcb.13419.
- [13] IPCC. (2021). *Climate Change 2021: The Physical Science Basis. Contribution of Working Group I to the Sixth Assessment Report of the Intergovernmental Panel on Climate Change; Intergovernmental Panel on Climate Change (IPCC)*, Geneva, Switzerland.
- [14] Azizi, H., Ebrahimi, H., Samani, H. M. V., & Khaki, V. (2021). Evaluating the effects of climate change on groundwater level in the Varamin plain. *Water Science and Technology: Water Supply*, 21(3), 1372–1384. doi:10.2166/ws.2021.007.
- [15] Ghazavi, R., & Ebrahimi, H. (2019). Predicting the impacts of climate change on groundwater recharge in an arid environment using modeling approach. *International Journal of Climate Change Strategies and Management*, 11(1), 88–99. doi:10.1108/IJCCSM-04-2017-0085.
- [16] Earman, S., & Dettinger, M. (2011). Potential impacts of climate change on groundwater resources - A global review. *Journal of Water and Climate Change*, 2(4), 213–229. doi:10.2166/wcc.2011.034.
- [17] Reinecke, R., Müller Schmied, H., Trautmann, T., Seaby Andersen, L., Burek, P., Flörke, M., Gosling, S. N., Grillakis, M., Hanasaki, N., Koutroulis, A., Pokhrel, Y., Thiery, W., Wada, Y., Yusuke, S., & Döll, P. (2021). Uncertainty of simulated groundwater recharge at different global warming levels: A global-scale multi-model ensemble study. *Hydrology and Earth System Sciences*, 25(2), 787–810. doi:10.5194/hess-25-787-2021.
- [18] Bouwer, H. (2002). Artificial recharge of groundwater: Hydrogeology and engineering. *Hydrogeology Journal*, 10(1), 121–142. doi:10.1007/s10040-001-0182-4.
- [19] Hassan, W. H., & Hashim, F. S. (2020). The effect of climate change on the maximum temperature in Southwest Iraq using HadCM3 and CanESM2 modelling. *SN Applied Sciences*, 2(9), 1494. doi:10.1007/s42452-020-03302-z.
- [20] Hussain, T. A., Ismail, M. M., & Al-Ansari, N. (2021). Simulation of the ground water flow in Karbala Governorate, Iraq. *Environmental Earth Sciences*, 80(5). doi:10.1007/s12665-021-09452-6.
- [21] Khalaf, R. M., Hussein, H. H., Hassan, W. H., Mohammed, Z. M., & Nile, B. K. (2022). Projections of precipitation and temperature in Southern Iraq using a LARS-WG Stochastic weather generator. *Physics and Chemistry of the Earth*, 128, 103224. doi:10.1016/j.pce.2022.103224.
- [22] Al-Mussawi, W. H. (2008). Kriging of groundwater level-a case study of Dibdiba Aquifer in area of Karbala-Najaf. *Journal of Karbala University*, 6(1), 170-182.
- [23] Ramadhan, A., Ali, M., & Al-Kubaisy, R. (2013). Evaluation of groundwater recharge in arid and semiarid regions (case study of Dibdiba formation in Karbala-Najaf plateau). *Iraqi Journal of Science*, 54(4), 902-910.

- [24] Al-Kubaisi, Q. Y., Al-Abadi, A. M., & Al-Ghanimy, M. A. (2018). Estimation of groundwater recharge by groundwater level fluctuation method of dibdibba aquifer at Karbala- Najaf plateau, central of Iraq. *Iraqi Journal of Science*, 59(4), 1899–1909. doi:10.24996/IJS.2018.59.4A.14.
- [25] Al-Dabbas, M., Khafaji, R. A., & Al-Jaberi, M. H. A. (2015). Impact of climate changes on the hydrogeological aquifers-case study Dibdiba aquifer at Karbala Najaf area, Iraq. *International Journal of Research in Science and Technology*, 5(3), 24–39.
- [26] Al-Ghanimy, M. A. (2018). Assessment of Hydrogeological Condition in Karbala—Najaf Plateau, Iraq. PhD Thesis, University of Baghdad, Baghdad, Iraq.
- [27] UNEP. (2000). Global warming environmental, report. United Nations Environment Programme (UNEP), Nairobi, Kenya.
- [28] Al-Kubaisi, Q. Y. (2004). Annual aridity index of type. 1 and type. 2 mode options climate classification. *Science Journal*, 45(1), 32–40.
- [29] Yeboah, K. A., Akpoti, K., Kabo-bah, A. T., Ofosu, E. A., Siabi, E. K., Mortey, E. M., & Okyereh, S. A. (2022). Assessing climate change projections in the Volta Basin using the CORDEX-Africa climate simulations and statistical bias-correction. *Environmental Challenges*, 6, 100439. doi:10.1016/j.envc.2021.100439.
- [30] Amognehegn, A. E., Nigussie, A. B., Adamu, A. Y., & Mulu, G. F. (2023). Analysis of future meteorological, hydrological, and agricultural drought characterization under climate change in Kessie watershed, Ethiopia. *Geocarto International*, 38(1), 2247377. doi:10.1080/10106049.2023.2247377.
- [31] Ghodoosipour, B. (2013). Three dimensional groundwater modeling in Laxemar-Simepevarp quaternary deposits. 13 41 TRITA-LWR Degree Project, Royal Institute of Technology (KTH), Stockholm, Sweden.
- [32] Toews, M. W. (2007). Modelling climate change impacts on groundwater recharge in a semi-arid region, southern Okanagan, British Columbia. Master Thesis, Simon Fraser University, Burnaby, Canada.
- [33] Niswonger, R. G., Prudic, D. E., & Regan, R. S. (2006). Documentation of the Unsaturated-Zone Flow (UZFI) Package for modeling Unsaturated Flow between the Land Surface and the Water Table with MODFLOW-2005. Techniques and Methods. United States Geological Survey (USGS), Reston, United States. doi:10.3133/tm6a19.
- [34] Al-Muqaddi, S. W. (2012). Groundwater investigation and modeling-western desert of Iraq. Ph.D. Thesis, Technische Universität Bergakademie Freiberg, Freiberg, Germany.
- [35] Mustafa, J. S., & Mawlood, D. K. (2024). Assessment of the Groundwater in Erbil Basin with Support of Visual MODFLOW. *Journal of Ecological Engineering*, 25(4), 203–227. doi:10.12911/22998993/184184.
- [36] Hosseinizadeh, A., Zarei, H., Akhondali, A. M., Seyedkaboli, H., & Farjad, B. (2019). Potential impacts of climate change on groundwater resources: A multi-regional modelling assessment. *Journal of Earth System Science*, 128(5). doi:10.1007/s12040-019-1134-5.
- [37] Geleta, C. D., & Gobosho, L. (2018). Climate change induced temperature prediction and bias correction in Finchaa watershed. *American-Eurasian Journal of Agricultural & Environmental Sciences*, 18, 324–337. doi:10.5829/idosi.ajeaes.2018.324.337.
- [38] Thornthwaite, C. W. (1948). An approach toward a rational classification of climate. *Geographical Review*, 38(1), 55–94. doi:10.2307/210739.
- [39] Moriasi, D. N., Arnold, J. G., Van Liew, M. W., Bingner, R. L., Harmel, R. D., & Veith, T. L. (2007). Model evaluation guidelines for systematic quantification of accuracy in watershed simulations. *Transactions of the ASABE*, 50(3), 885–900. doi:10.13031/2013.23153.
- [40] Dragoni, W., & Sukhija, B. S. (2008). Climate change and groundwater: A short review. *Geological Society Special Publication*, 288, 1–12. doi:10.1144/SP288.1.